BRG1/BRM-associated factor complex subunit diversity promotes temporally distinct gene expression programs in cardiogenesis

Swetansu K. Hota[1,2], Jeffrey R. Johnson[1,3], Erik Verschueren[1,3], Yiwen Zhu[4,5], Xin Sun[6,7,10], Len A. Pennacchio[4,5], Janet Rossant[6,7], Nevan J. Krogan[1,3], and Benoit G. Bruneau[1,2,8,9]

1. Gladstone Institutes, San Francisco, CA, 94158 USA

2. Roddenberry Center for Stem Cell Biology and Medicine at Gladstone, San Francisco, CA 94158, USA

3. Department of Cellular and Molecular Pharmacology, University of California San Francisco, San Francisco, CA 94158

4. Genomics Division, Lawrence Berkeley National Laboratory, Berkeley, CA 94720, USA.

5. United States Department of Energy, Joint Genome Institute, Walnut Creek, CA 94598, USA.

6. Program in Developmental and Stem Cell Biology, The Hospital for Sick Children, Toronto, ON, M5G 1X8 Canada

7. Department of Molecular Genetics, University of Toronto, Toronto, ON M5S 1A8 Canada

8. Department of Pediatrics, University of California, San Francisco, CA 94143 USA

9. Cardiovascular Research Institute, University of California, San Francisco, CA 94158 USA

10. Current address: Department of Physiology, Anatomy and Genetics, University of Oxford.

Correspondence to B.G.B (benoit.bruneau@gladstone.ucsf.edu)

SUMMARY

Chromatin remodeling complexes instruct cellular differentiation and lineage specific transcription. However, the underlying mechanism is unclear. Here, using immunoprecipitation

with mass spectrometry (IP-MS), we determined the dynamic composition of the BRG1/BRM associated factor (BAF) complexes during mammalian cardiac differentiation, and identified BAF60c (SMARCD3) and BAF170 (SMARCC2) as subunits enriched in cardiac precursors (CP) and cardiomyocytes (CM). The catalytic subunit *Brg1* has a specific role in CPs to initiate cardiac gene expression programs and repress non-cardiac fates, a role shared by *Baf60c* and *Baf170*. In CMs, BAF60c and BAF170 are found in BRG1 and BRM-associated complexes, and are essential for maintaining the cardiac program, largely by repressing non-cardiac gene expression. BAF60c and BAF170 both modulate BAF complex composition and stoichiometry. In CM, BAF170 facilitates expulsion of a subset of BRG1-containing complexes near genes regulating post-transcriptional and epigenetic modification, as opposed to those evicted independent of BAF170 that regulate transcription, growth and development. Thus, BAF complexes use varied interdependent mechanisms to direct temporal gene expression programs in cardiogenesis.

INRODUCTION

Cell differentiation and organogenesis are regulated by the precise transcriptional output of a coordinated gene network. During mammalian development, gene expression programs are spatially and temporally controlled with specific sets of genes being expressed while others are poised or repressed in a developmental stage dependent manner. Delineating the factors that control these crucial decision points is essential to understand the developmental control of gene regulation.

Transcription factor (TF) activity regulates transcriptional output, and is intimately influenced by the underlying chromatin architecture. Chromatin remodeling complexes alter chromatin structure to regulate transcription. These are multi-subunit protein complexes that utilize energy from ATP hydrolysis to alter the histone DNA contact in nucleosomes, the basic unit of

chromatin (Clapier and Cairns 2009; Bartholomew 2014; Zhou et al. 2016). The BRG1/ BRM associated factor (BAF) chromatin remodeling complexes are 15-18 subunit protein complexes. Brahma (BRM) or Brahma-related gene 1 (BRG1) are the mutually exclusive catalytic subunits that associate with several other structural subunits and their isoforms, to from diverse BAF complexes and serve specific functions in widely different cell types and developmental processes (Wang et al. 1996b; Ho and Crabtree 2010; Hota and Bruneau 2016). It is proposed that this diversity in BAF complexes is tailored to provide a unique surface to bind TFs leading to tissue specific function. How BAF complexes regulate transcription of specific developmental processes is not clearly understood.

In the developing heart, various subunits of the BAF complex are involved in aspects of cardiac development including early cardiac specification, heart tube looping, cardiomyocyte commitment, ventricular chamber morphogenesis, interventricular septum formation and trabeculation (Devine et al. 2014; Lange et al. 2008; Cai et al. 2013; He et al. 2014; Takeuchi et al. 2011; Stankunas et al. 2008). It is not known if these subunits function individually, or assemble together as one or more specialized cardiac BAF complex(es) with shared or distinct function.

Here, we define dynamic BAF complex composition during mouse cardiomyocyte differentiation. We identify the BAF subunits BAF60c and BAF170 as enriched in cardiac precursors and cardiomyocytes. BRG1 initiates cardiac gene expression programs in precursor cells, a role shared by BAF60c and BAF170, which also maintain the cardiac program to facilitate cardiomyocyte differentiation. BAF60c and BAF170 also regulate BAF complex composition and stoichiometry. Further, we find that BAF170 facilitates dissociation of BRG1 complexes from their binding sites upon cardiomyocyte differentiation. These results reveal the instructive nature

that specific combination of BAF subunits attain to dictate functional outcomes during lineage commitment and differentiation.

RESULTS

BRG1 complex shows dynamic composition during cardiomyocyte differentiation

To model early heart development, we differentiated mouse embryonic stem cells (mESCs) to cardiac troponin positive (cTnT+) beating cardiac myocytes (Kattman et al. 2011; Wamstad et al. 2012). We regularly obtained 75 -90% cTnT+ beating cardiac myocytes as measured by flow cytometry. BAF complex members have been implicated in TF interaction and cardiac development (Hota and Bruneau 2016; Bevilacqua et al. 2014), however we have limited knowledge on how BAF subunits change during cardiogenesis (Singh and Archer 2014). In order to understand the composition of BAF complexes, we immunoprecipitated BRG1 using a strain that contains triple FLAG tag at the C-terminus of one of the endogenous *Brg1* alleles (Attanasio et al. 2014), at five different stages of cardiac differentiation: ES cells (ESC), embroid bodies (EB), mesoderm (MES), cardiac progenitor (CP) and cardiac myocytes (CM) (Fig. 1A). BAF complexes isolated from ESCs and separated on SDS PAGE (Fig. 1B) shows protein profiles similar to other reports (Ho et al. 2009b). Mass-spectrometric analyses of protein complexes isolated from five different stages of cardiac differentiation identified the composition of the BAF complex at these stages (Fig. 1C; Supplemental Table S1). BAF complexes isolated form ES cells were enriched for subunits BRD9, GLTSCR1l, BCL7b&c, BAF155 and BAF60a, consistent with previous reports (Ho et al. 2009b; Kadoch and Crabtree 2013). Similarly, we identified proteins enriched at mesoderm (PDE4D, CRABP2), CP (RPL7a, Polybromo-1, BAF47, BRD7 and BAF45a) and CM stages (BAF170, BAF60c, BAF57, SS18l1, BAF45c and CC2D1B). Identification of these enriched subunits revealed that BAF complex changes its composition during cardiac differentiation and BAF subunits switch from one isoform to other (for example, BAF60a in ES BAF complexes is replaced by BAF60c in cardiac BAF complexes)

or to a different protein (BAF155 in ES cells to BAF170 in cardiac cells). We confirmed the switch in BAF155 in ES BAF to more abundant BAF170 in cardiac cells and appearance of BAF60c only in cardiac cell lineages during differentiation by western blot (Fig. 1D). Thus, BAF complexes have dynamic subunit composition and enrich for specific subunits in cardiac lineages.

Cardiac enriched BAF subunits form distinct cardiac BAF complexes

To further understand the composition of cardiac enriched BAF complexes, we immunoprecipitated endogenous FLAG tagged BAF170 or BAF60c at different stages of cardiac differentiation and analyzed by mass spectrometry. An untagged cell line processed identically served as negative control. BAF complexes isolated using BAF170 as the bait protein revealed that at each of the ES, EB and MES stages the protein abundance is too low (Fig. 1E). This is consistent with the expression of *Baf170*, which only peaks at the CP stage of differentiation (Supplemental Fig. S1A). Most of the BAF subunits enriched at the CP and CM stages using BRG1 as the bait protein were also enriched using BAF170 as the bait (Fig. 1E). In addition, we detected WDR5, PKP1 and BRM in the BAF170-FLAG purification. WDR5 was also present at lower enrichment in the BRG1 complexes (Supplemental Fig. S1B). We do not detect PKP1 or BRM in BRG1-FLAG purifications, indicating that BAF170 may specifically interact with these subunits, and consistent with BRG1 and BRM being mutually exclusive BAF complex catalytic subunits (Wang et al. 1996a). IP-MS revealed that BAF170 begins to associate with BRM at CP and BRM association with BAF170 increases in CM (Fig. 1E). BAF complexes isolated using FLAG-BAF60c were similar to those of BAF170-FLAG isolated complex (Fig. 1F). Again, we detected both BRG1 and BRM, indicating that BAF170 and BAF60c containing complexes swap out BRG1 for BRM as their primary catalytic subunit during cardiac differentiation.

To understand if changes in subunit abundance are due to transcriptional changes of that particular subunit or due to its association with the BAF complex, we plotted normalized FPKM values of these subunits at four stages of differentiation and found that while transcriptional changes correlate with BAF association in some cases (for example BAF60c, BAF170), in others it is independent of expression (for example, WDR5 is expressed mostly in ESC, while it associates with BAF complexes only in CMs) (Supplemental Fig. S1A,B).

Dynamic subunit composition does not affect BAF complex activity *in vitro*

We investigated if differentiation stages specific changes in composition affected biochemical activities of BAF complexes by performing ATP hydrolysis and nucleosome repositioning assays (Hota and Bartholomew 2012). *In-vitro* reconstituted mononucleosomes (Lusser and Kadonaga 2004; Lowary and Widom 1998) were incubated with equal amount of BRG1 isolated complex from all the five stages of differentiation with constant amount of ATP from 30s to 2hrs and resolved in a native polyacrylamide gel (Fig. 2A). Electrophoretic mobility shift assay revealed that BAF complexes isolated from ES cells (esBAF) could shift centrally positioned nucleosomes towards the end of the DNA fragment, as observed by the faster migration in native PAGE (Fig. 2A, lanes 1-5). BAF complexes isolated from other stages of differentiation (ebBAF, mesBAF, cpBAF and cmBAF) could also similarly shift centrally located nucleosome towards end of the DNA after incubation for various length of time (Fig. 2A, compare lanes 1-5 to 6-10, 11-15, 16-20 and 21-25 and Fig. 2B). This indicates that altered subunits in BAF complexes do not significantly contribute toward repositioning of *in vitro* reconstituted nucleosomes. We tested the abilities of these complexes to hydrolyze ATP in presence of nucleosome and found that BAF complexes isolated from different stages of differentiation could similarly hydrolyze ATP to ADP and free phosphate (Fig. 2C). Thus, although cell-type specific BAF complexes show alteration in subunit composition and enrichment of specific subunits, it

appears that these subunits do not engage in regulating the ATP hydrolysis and nucleosome mobilizing activities of BAF complexes.

Brg1 initiates cardiac gene expression programs during cardiomyocyte differentiation

To understand how changing BAF complex subunit composition transcriptionally affects cardiac differentiation, we examined the role of the catalytic subunit BRG1 and cardiac enriched subunits BAF60c and BAF170 during cardiomyocyte differentiation. First, we conditionally deleted *Brg1* (also known as *Smarca4*) using an ES cell strain that flanks exon 17 and 18 of *Brg1* with loxP sites and expresses creER under β-actin promoter (*Brg1*$^{flox/flox}$;βActin creER; Brg1KO) (Ho et al. 2011). Addition of 4-hydroxytamoxifen (4OHT) to culture medium for 48hrs effectively deleted these exons and reduced BRG1 protein levels to undetectable levels (Alexander et al. 2015). The effect of *Brg1* deletion at CP and CM stages of differentiation on transcription was evaluated by RNA sequencing (RNASeq). Deletion of *Brg1* deregulated a total of 545 genes at CP and 125 genes at CM stage of differentiation (p <0.05, ± 1.5 fold), indicating a declining role of *Brg1* during the cardiomyocyte stage, consistent with its reduced expression at this stage (Fig. 3; Supplemental Fig. S1A). In CP, of the 545 deregulated genes, 197 (36.1%) and 348 (63.9%) were significantly up or down regulated respectively, indicating a dual role of BRG1 in repression and activation of genes (Fig. 3A). Gene set enrichment analysis (GSEA) (Subramanian et al. 2005) revealed that genes down regulated in absence of BRG1 correlated more with genes upregulated in CP over mesoderm (Supplemental Fig. S2A**,** left panel), indicating that BRG1 is an activator of a CP gene expression program. No such correlation was found for BRG1-repressed genes in CPs (Supplemental Fig. S2A**,** right panel). Consistent with the GSEA results, gene ontology (GO) term enrichment analyses revealed that BRG1 activates genes involved in sarcomere organization and assembly and are essential components of cardiac cell fate establishment (Fig. 3B). Of note, BRG1 is essential for the immediate activation of these lineage-specific genes, in anticipation of the final differentiation status of the cells.

Thus, BRG1-associated complexes prime the cell-type specific differentiation of cardiac precursors.

In cardiomyocytes, loss of BRG1 deregulated only 125 genes with roughly equal number of genes being activated (48%) or repressed (52%) (Fig. 3C). Although BRG1 activated genes correlated with CM (Supplemental Fig. S2B) gene ontology (GO) biological processes did not significantly enrich for any term (Fig. 3D) indicating BRG1 has minimal role in cardiac myocytes, consistent with in vivo data (Hang et al. 2010).

Cardiac enriched BAF subunits BAF170 and BAF60c facilitate cardiomyocyte differentiation

As altered subunit composition during cardiac differentiation did not affect ATPase or nucleosome repositioning abilities of BAF complexes, we investigated how cardiac enriched subunits regulate gene expression programs. We created BAF60c or BAF170 KO ES cell lines by TALEN or CRISPR mediated disruption of each gene and confirmed the clones by PCR, DNA sequencing and western blot (Supplemental Fig. S3A, S4A). ES cells lacking BAF60c or BAF170 undergo normal cardiac differentiation as observed by beating cardiac cells, immunostaining and intracellular FACS analysis of cardiac troponin T (cTnT). To understand the contribution of these subunits towards cardiac cell function and maturation and to compare the gene expression profile of cells lacking BAF170 or BAF60c to those lacking BRG1, we collected cells at CP and CM stages and performed RNASeq.

At CP, in absence of BAF60c, a total of 474 genes (p-value <0.05, ± 1.5-fold) were deregulated of which 215 (45.4%) were down regulated and 259 (54.6%) were upregulated (Supplemental Fig. S3B). while a total of 382 genes are deregulated in absence of BAF170, of which 192 (50.2%) were down regulated and 190 (49.8%) were upregulated (Supplemental Fig. S4B).

Gene ontology analyses revealed that BRG1 and BAF60c share common function in activating genes involved in muscle tissue morphogenesis, cardiac cell development and cardiac muscle contraction while repressing skeletal system and limb morphogenesis in CPs (Fig. 3B; Supplemental Fig. S3C). Genes regulated (largely repressed) by BAF170 are mostly involved in skeletal system morphogenesis and pattern specification (Supplemental Fig. S4C). In contrast, BAF60C regulated a large number of genes in cardiomyocytes (2646), repressing 72% of genes and activating 28% of these genes (Supplemental Fig. S3D, S3E). Although BAF170 regulated 574 genes in cardiomyocytes, a large percentage (63%) were up-regulated in absence of BAF170 (Supplemental Fig. S4D, S4E). These results indicate a largely repressive function of these cardiac enriched subunits in gene regulation.

Overall comparison of the gene expression changes in CPs and CMs lacking BRG1, BAF60c, or BAF170 show that BRG1, BAF60c and BAF170 have shared functions in CP gene expression, but that in CPs and CMs BAF60c and BAF170 repress a cohort of genes independent of BRG1 (Fig. 4A,4B). This clearly indicates divergent role of these two subunits from BRG1, suggesting their association in a different BAF complex or potential independent function outside of BAF complex. In line with these observation, we observed decreasing overlap between genes regulated by BRG1, BAF60c and BAF170 in CMs (Fig. 4C, 4D). Thus, varied but regulated combinations of subunits in BAF complexes regulate the transcriptional outcome of specific stages of development.

Both BAF170 and BAF60c regulate BAF complex stoichiometry

As both BAF60c and BAF170 has critical roles in transcriptional regulation of cardiac differentiation, we wished to understand the nature of BAF complexes formed in absence of these cardiac enriched subunits. Toward this goal, we isolated BAF complexes via immunoaffinity purification of FLAG tagged BRG1 protein from strains lacking BAF60c or

BAF170 at CP and CM. SDS PAGE revealed increased stability of BRG1-containing complexes in BAF170 KO CMs (Fig. 5A**,** compare lanes 8,9 and lanes 10,11 to Fig. 1B, lane 5 to lane 6). It appears that the decrease in levels of BRG1 band intensity from CP to CM is greatly minimized by lack of BAF170, indicating greater stability of BRG1 complex. Mass spectrometric analyses of these complexes revealed significant differences in subunit composition in the absence of BAF170 or BAF60c (Fig. 5B,5C). In CPs, BAF complexes lacking BAF170 had decreased association of BCL7a BAF45d, BAF60c, BAF47 and BAF53a, and were enriched for BAF45c, CREST and BAF180. In CMs, BAF complexes lacking BAF170 showed reduced association with BAF60c and increased association with BAF155 and BAF60b (Fig. 5B; Supplemental Fig S5A, S5B). Similarly, we observed alterations of subunits composition at CP and increased association of different subunits with BAF complex lacking BAF60c in cardiac myocytes (Fig. 5C; Supplemental Fig. S5A, S5B). The altered complexes formed are not due to changes in the transcriptional level of BAF subunits (Supplemental Fig. S5C).

These results suggest that a fine balance exists in the composition of the BAF complex and perturbation of one subunit extends to the stoichiometry of association of other subunits in the complex. It further indicates that different subunits or isoforms substitute for the absence of one or more subunits. For example, both BAF60a and BAF60b substitute for the lack of BAF60c, and depletion of BAF45c is balanced by enrichment of BAF45a (Supplemental Fig. S5B). These results emphasize that subunit switching and substitution in BAF complex composition could be an important mechanism in cardiac lineage specification.

BRG1 binding correlates well with sites of cardiac transcription factor binding

To understand the potential mechanisms by which cardiac enriched subunits BAF60c and BAF170 regulate gene expression, and to distinguish between the direct and indirect role of BRG1 in gene regulation, we evaluated genome-wide BRG1 chromatin occupancy by chromatin

immunoprecipitation using an antibody against BRG1 followed by sequencing of immunoprecipitated DNA (ChIP-Seq) in WT and cells lacking BAF60c or BAF170. We could not detect BRG1 occupancy in CMs, presumably due to the low levels of protein at this stage. In CPs, BRG1 was bound to both transcriptional start sites (TSS) and active enhancer regions marked by acetylation of lysine 27 residue of H3 (Wamstad et al. 2012) (Fig. 6A). TSS of genes deregulated (up or down regulated) in the absence of BRG1 show significant binding of BRG1 (Fig. 6B). For example, the upstream regulatory regions of BRG1 activated genes *Tbx5* and *Myocd* and promoter regions of the repressed gene *Rdh10* show significant BRG1 binding over input control (Fig. 6C). We found 4791 significant BRG1 binding regions (Supplemental Fig. S6A). About 60% of BRG1 binding sites are associated with the promoter region and rest are in distal regulatory region and are associated with 5274 genes within one megabase of BRG1 binding sites (Supplemental Fig. S6B, S6C). Of the 545 *Brg1KO* deregulated genes in CPs, 21.9% of BRG1 activated and 20.9% of the BRG1 repressed genes overlapped with genes nearest to a BRG1 binding site indicating that these genes may be putative direct targets of BRG1 (Supplemental Fig. S6D). BRG1 activated direct targets enriched for biological processes like cardiac muscle and tissue development and contraction, and circulatory system processes. Target genes that are repressed by BRG1 are enriched for biological processes including embryonic hind limb and forelimb morphogenesis and skeletal system development (Fig. 6D). We selected active enhancer regions based on their enrichment of acetylation marks on lysine 27 residue of histone H3 in CPs (Wamstad et al. 2012). Several BRG1 regulated genes (23.6% of BRG1 activated and 16.8% of BRG1 repressed genes) intersected with genes nearest to enhancer marks (Supplemental Fig S6E). BRG1 activated genes near to the enhancer marks enriched for processes such as muscle contraction, acto-myosin structure organization and cardiac tissue morphogenesis whereas repressed genes near enhancer marks were enriched for negative regulation of endothelial cell proliferation, biosynthetic processes and regionalization (Fig. 6E). These results show that putative directs of BRG1 are involved in

facilitation of cardiac gene expression programs while preventing other developmental programs including embryonic limb development.

Cardiac transcription factors (TFs) often recruit and use chromatin remodeling machinery to reorganize chromatin and regulate transcription (Lickert et al. 2004; Takeuchi and Bruneau 2009; Takeuchi et al. 2011). To evaluate a potential BRG1-TF collaboration during cardiac differentiation we searched for TF motifs in BRG1 binding regions associated with both BRG1 activated and repressed genes using Homer motif enrichment analysis (Heinz et al. 2010). BRG1 activated regions were found to be associated predominantly with GATA motifs whereas BRG1 repressed regions were associated with T-box motifs among others (Fig. 6F,6G). Consistent with these observations BRG1 binding sites correlated well with GATA4 and TBX5 binding sites in cardiac precursors (Fig. 6H,6I) (Luna-Zurita et al. 2016). These results indicate that BRG1 or other BRG1 associated factors likely interact with cardiac TFs to regulate gene expression during cardiac lineage commitment, as predicted from gain of function experiments (Lickert et al. 2004; Takeuchi and Bruneau 2009).

BAF170 facilitates temporal BRG1 dissociation from the genome

We explored the possibility that BAF60c or BAF170 help direct the genomic localization of BRG1. In CPs, BRG1 binds to a set of 4791 sites (Supplemental Fig. S6A) and are largely unaffected in absence of BAF170 (Fig. 7A). BRG1 binding at these site is severely reduced in cardiomyocytes in WT and cells lacking BAF60c, presumably due to the reduced predominance of a BRG1-containing complex. However, in the absence of BAF170, BRG1 binding at a large subset of these sites is retained in cardiomyocytes (Fig. 7B). This retention is reflected by stabilization of a BRG1 containing complex in CMs lacking BAF170 (Fig. 5A), perhaps due to posttranscriptional stabilization and/or retention of available BRG1 in a complex. Further, analysis revealed that genes near these sites are involved in chromosome organization,

epigenetic modification of chromatin and post-transcriptional regulation of gene expression (Supplemental Fig S7A, S7B). On the other hand at a small subset of sites (21%, 1019 of 4791), BRG1 was evicted independent of BAF170 in CM (Supplemental Fig. S7A). Genes near these sites are involved in regulation of embryonic growth and morphogenesis and RNA pol II mediated transcription (Supplemental Fig. S7C). These surprising results suggest that recruitment of BRG1-inclusive complexes is regulated by cardiac specific subunits, and that concomitant dynamic expulsion of the complex is also highly regulated by similar processes.

DISCUSSION

BRG1 containing complexes respond to and modulate lineage decisions and differentiation in cardiac development by incorporating specific subunits at discrete stages. These specialized BAF complexes regulate distinct gene expression programs to drive cardiogenesis while simultaneously repressing alternate non-cardiac developmental programs. Our results suggest that BAF complexes utilize multiple interdependent mechanisms including switching subunits or isoforms, regulating subunit stoichiometry, altering BRG1 recruitment, and expulsion strategies, to modulate dynamics of cardiac differentiation. This unanticipated complexity of chromatin complex regulation emerges as a critical determinant of developmental trajectories.

Subunit composition switching of chromatin remodeling complexes have been reported during neural development (Lessard et al. 2007; Yoo et al. 2009; Nitarska et al. 2016) . and skeletal myogenesis (Saccone et al. 2014; Goljanek-Whysall et al. 2014). During myogenic differentiation, BAF60c expression is facilitated over the alternative isoforms BAF60a and BAF60b, which are post-transcriptionally repressed by myogenic microRNAs. The subunit switches we describe for BAF complexes during cardiomyocyte differentiation involve different subunits than in neural cells but if such a microRNA mediated repression mechanism selects BAF60c is not known. Importantly, we show that BAF complexes at different stages of cardiac

differentiation form specific complexes to activate or repress specific transcriptional programs. In addition, we determine that the presence of specific BAF subunits greatly dictates the overall composition, and therefore function, of the complex.

The cardiac enriched subunits BAF60c and BAF170 are primarily associated with BRG1 in CPs, but also associate with BRM in CMs, indicating a broader diversity of BAF complexes in later stages of differentiation. Paradoxically, the continued roles played by BAF60c and BAF170 are intriguing considering the reduced role of BRG1 in later stages of cardiac differentiation, and the apparent absence of a developmental or postnatal cardiac phenotype in BRM null mice (Reyes et al. 1998). It has been suggested that BAF60c may function independently from the BAF complex (Forcales et al. 2012; Wang et al. 2013), although there is no evidence for this in cardiac cells. It is also possible that the previously reported BRM deletion allele is not a complete null (Thompson et al. 2015). We are investigating both of these avenues.

BRG1 binding to genomic sites in CP and putative BRG1 direct targets have critical roles in promotion of cardiac gene expression programs while repressing non-cardiac fate. BRG1 binding is greatly reduced in CM indicating diminished BRG1 function. Our finding that, BAF170 largely helps BRG1 dissociation from genome indicates a potential mechanism of BAF170 mediated gene regulation during differentiation. How BAF170 regulate genomic expulsion of BRG1 is currently not understood, but association of BAF170 with BRM containing complexes in CM might evict BRG1 from BAF complexes as both these subunits are mutually exclusive. Further, concomitant increase in BAF170 and decrease of BAF155 association with BRG1 containing complexes during cardiac differentiation might make BRG1 prone to post-transcriptional modification and proteasome mediated degradation, as BAF155 is known to stabilize BRG1 containing complexes (Sohn et al. 2007). Consistently, we observe BRG1 complex stabilization in absence of BAF170 in CMs (Fig. 5A).

In conclusion, our study identifies morphing combinations of very specific BAF subunits that form and change subunit compositions during cardiac differentiation, and drive stage-specific cardiac gene expression programs. Genetic dissection of individual subunit contribution clearly unveils a profound and specific function of individual BAF complex subunits. How BAF chromatin remodelers with different subunit composition provide specificity to gene expression programs will be the focus of future studies.

Author Contribution

Project design and direction: B.G.B. ES cell engineering, in vitro differentiation, complex isolation, gene expression analysis, data analysis: S.K.H. BAF60c FLAG allele generation: X.S, under direction of B.G.B and J.R. Mass spectrometry and analysis: J.R.J, E.V., under direction of N.J.K. Manuscript writing: S.K.H and B.G.B with contribution from all authors.

Acknowledgements

We thank A. Williams and S. Thomas (Gladstone Bioinformatics Core) for data analysis, L. Ta and J. McGuire (Gladstone Genomics Core) for RNAseq library preparation, and G. Howard for editing. RNAseq (258R1 and 420R) and ChIPSeq (451R) data are publicly available at https://b2b.hci.utah.edu/gnomex/ and GEO (accession number). This work was supported by grants from the NIH/NHLBI (R01HL085860, P01HL089707**,** Bench to Bassinet Program UM1HL098179), the California Institutes of Regenerative Medicine (RN2-00903), and the Lawrence J. and Florence A. DeGeorge Charitable Trust/American Heart Association Established Investigator Award (B.G.B), and postdoctoral fellowships from the American Heart Association (13POST17290043) and Tobacco Related Disease Research Program (22FT-0079)

to S.K.H. L.A.P. was supported by NHLBI grant R24HL123879, and NHGRI grants R01HG003988, and UM1HG009421, and research was conducted at the E.O. Lawrence Berkeley National Laboratory was performed under Department of Energy Contract DE-AC02-05CH11231, University of California. This work was also supported by an NIH/NCRR grant (C06 RR018928) to the J. David Gladstone Institutes and by The Younger Family Fund (B.G.B.).

References

Abmayr SM, Yao T, Parmely T, Workman JL. 2006. Preparation of nuclear and cytoplasmic extracts from mammalian cells. *Curr Protoc Mol Biol* **Chapter 12**: Unit 12.1–12.1.10.

Alexander JM, Hota SK, He D, Thomas S, Ho L, Pennacchio LA, Bruneau BG. 2015. Brg1 modulates enhancer activation in mesoderm lineage commitment. *Development* **142**: 1418–1430.

Attanasio C, Nord AS, Zhu Y, Blow MJ, Biddie SC, Mendenhall EM, Dixon J, Wright C, Hosseini R, Akiyama JA, et al. 2014. Tissue-specific SMARCA4 binding at active and repressed regulatory elements during embryogenesis. *Genome Research* **24**: 920–929.

Bartholomew B. 2014. Regulating the chromatin landscape: structural and mechanistic perspectives. *Annu Rev Biochem* **83**: 671–696.

Bevilacqua A, Willis MS, Bultman SJ. 2014. SWI/SNF chromatin-remodeling complexes in cardiovascular development and disease. *Cardiovasc Pathol* **23**: 85–91.

Cai W, Albini S, Wei K, Willems E, Guzzo RM, Tsuda M, Giordani L, Spiering S, Kurian L, Yeo GW, et al. 2013. Coordinate Nodal and BMP inhibition directs Baf60c-dependent cardiomyocyte commitment. *Genes & Development* **27**: 2332–2344.

Choi M, Chang C-Y, Clough T, Broudy D, Killeen T, MacLean B, Vitek O. 2014. MSstats: an R package for statistical analysis of quantitative mass spectrometry-based proteomic experiments. *Bioinformatics* **30**: 2524–2526.

Clapier CR, Cairns BR. 2009. The Biology of Chromatin Remodeling Complexes. *Annu Rev Biochem* **78**: 273–304.

Cong L, Ran FA, Cox D, Lin S, Barretto R, Habib N, Hsu PD, Wu X, Jiang W, Marraffini LA, et al. 2013. Multiplex genome engineering using CRISPR/Cas systems. *Science* **339**: 819–823.

Cox J, Mann M. 2008. MaxQuant enables high peptide identification rates, individualized p.p.b.-range mass accuracies and proteome-wide protein quantification. *Nat Biotechnol* **26**: 1367–1372.

Devine WP, Wythe JD, George M, Koshiba-Takeuchi K, Bruneau BG. 2014. Early patterning and specification of cardiac progenitors in gastrulating mesoderm. *Elife* **3**: –.

Forcales SV, Albini S, Giordani L, Malecova B, Cignolo L, Chernov A, Coutinho P, Saccone V, Consalvi S, Williams R, et al. 2012. Signal-dependent incorporation of MyoD-BAF60c into Brg1-based SWI/SNF chromatin-remodelling complex. *The EMBO Journal* **31**: 301–316.

Giorgetti L, Galupa R, Nora EP, Piolot T, Lam F, Dekker J, Tiana G, Heard E. 2014. Predictive polymer modeling reveals coupled fluctuations in chromosome conformation and transcription. *Cell* **157**: 950–963.

Goljanek-Whysall K, Mok GF, Fahad Alrefaei A, Kennerley N, Wheeler GN, Münsterberg A. 2014. myomiR-dependent switching of BAF60 variant incorporation into Brg1 chromatin remodeling complexes during embryo myogenesis. *Development* **141**: 3378–3387.

Hang CT, Yang J, Han P, Cheng H-L, Shang C, Ashley E, Zhou B, Chang C-P. 2010. Chromatin regulation by Brg1 underlies heart muscle development and disease. *Nature* **466**: 62–67.

He L, Tian X, Zhang H, Hu T, Huang X, Zhang L, Wang Z, Zhou B. 2014. BAF200 is required for heart morphogenesis and coronary artery development. ed. L. Chen. *PLoS ONE* **9**: e109493.

Heinz S, Benner C, Spann N, Bertolino E, Lin YC, Laslo P, Cheng JX, Murre C, Singh H, Glass CK. 2010. Simple combinations of lineage-determining transcription factors prime cis-regulatory elements required for macrophage and B cell identities. *Molecular Cell* **38**: 576–589.

Ho L, Crabtree GR. 2010. Chromatin remodelling during development. *Nature* **463**: 474–484.

Ho L, Jothi R, Ronan JL, Cui K, Zhao K, Crabtree GR. 2009a. An embryonic stem cell chromatin remodeling complex, esBAF, is an essential component of the core pluripotency transcriptional network. *Proc Natl Acad Sci USA* **106**: 5187–5191.

Ho L, Miller EL, Ronan JL, Ho WQ, Jothi R, Crabtree GR. 2011. esBAF facilitates pluripotency by conditioning the genome for LIF/STAT3 signalling and by regulating polycomb function. *Nature Cell Biology* **13**: 903–913.

Ho L, Ronan JL, Wu J, Staahl BT, Chen L, Kuo A, Lessard J, Nesvizhskii AI, Ranish J, Crabtree GR. 2009b. An embryonic stem cell chromatin remodeling complex, esBAF, is essential for embryonic stem cell self-renewal and pluripotency. *Proc Natl Acad Sci USA* **106**: 5181–5186.

Hota SK, Bartholomew B. 2012. Approaches for studying nucleosome movement by ATP-dependent chromatin remodeling complexes. *Methods Mol Biol* **809**: 367–380.

Hota SK, Bhardwaj SK, Deindl S, Lin Y-C, Zhuang X, Bartholomew B. 2013. Nucleosome mobilization by ISW2 requires the concerted action of the ATPase and SLIDE domains. *Nature Structural & Molecular Biology* **20**: 222–229.

Hota SK, Bruneau BG. 2016. ATP-dependent chromatin remodeling during mammalian

development. *Development* **143**: 2882–2897.

Kadoch C, Crabtree GR. 2013. Reversible disruption of mSWI/SNF (BAF) complexes by the SS18-SSX oncogenic fusion in synovial sarcoma. *Cell* **153**: 71–85.

Kattman SJ, Witty AD, Gagliardi M, Dubois NC, Niapour M, Hotta A, Ellis J, Keller G. 2011. Stage-specific optimization of activin/nodal and BMP signaling promotes cardiac differentiation of mouse and human pluripotent stem cell lines. *Cell Stem Cell* **8**: 228–240.

Kim D, Pertea G, Trapnell C, Pimentel H, Kelley R, Salzberg SL. 2013. TopHat2: accurate alignment of transcriptomes in the presence of insertions, deletions and gene fusions. *Genome Biol* **14**: R36.

Lange M, Kaynak B, Forster UB, Tönjes M, Fischer JJ, Grimm C, Schlesinger J, Just S, Dunkel I, Krueger T, et al. 2008. Regulation of muscle development by DPF3, a novel histone acetylation and methylation reader of the BAF chromatin remodeling complex. *Genes & Development* **22**: 2370–2384.

Langmead B, Trapnell C, Pop M, Salzberg SL. 2009. Ultrafast and memory-efficient alignment of short DNA sequences to the human genome. *Genome Biol* **10**: R25.

Lessard J, Wu JI, Ranish JA, Wan M, Winslow MM, Staahl BT, Wu H, Aebersold R, Graef IA, Crabtree GR. 2007. An Essential Switch in Subunit Composition of a Chromatin Remodeling Complex during Neural Development. *Neuron* **55**: 201–215.

Liao Y, Smyth GK, Shi W. 2014. featureCounts: an efficient general purpose program for assigning sequence reads to genomic features. *Bioinformatics* **30**: 923–930.

Lickert H, Takeuchi JK, Both Von I, Walls JR, McAuliffe F, Adamson SL, Henkelman RM, Wrana JL, Rossant J, Bruneau BG. 2004. Baf60c is essential for function of BAF chromatin remodelling complexes in heart development. *Nature* **432**: 107–112.

Lowary PT, Widom J. 1998. New DNA sequence rules for high affinity binding to histone octamer and sequence-directed nucleosome positioning. *J Mol Biol* **276**: 19–42.

Luna-Zurita L, Stirnimann CU, Glatt S, Kaynak BL, Thomas S, Baudin F, Samee MAH, He D, Small EM, Mileikovsky M, et al. 2016. Complex Interdependence Regulates Heterotypic Transcription Factor Distribution and Coordinates Cardiogenesis. *Cell* **164**: 999–1014.

Lusser A, Kadonaga JT. 2004. Strategies for the reconstitution of chromatin. *Nat Meth* **1**: 19–26.

Nitarska J, Smith JG, Sherlock WT, Hillege MMG, Nott A, Barshop WD, Vashisht AA, Wohlschlegel JA, Mitter R, Riccio A. 2016. A Functional Switch of NuRD Chromatin Remodeling Complex Subunits Regulates Mouse Cortical Development. *Cell Rep* **17**: 1683–1698.

O'Geen H, Echipare L, Farnham PJ. 2011. Using ChIP-seq technology to generate high-resolution profiles of histone modifications. *Methods Mol Biol* **791**: 265–286.

Reyes JC, Barra J, Muchardt C, Camus A, Babinet C, Yaniv M. 1998. Altered control of cellular proliferation in the absence of mammalian brahma (SNF2alpha). *The EMBO Journal* **17**:

6979–6991.

Robinson MD, McCarthy DJ, Smyth GK. 2010. edgeR: a Bioconductor package for differential expression analysis of digital gene expression data. *Bioinformatics* **26**: 139–140.

Saccone V, Consalvi S, Giordani L, Mozzetta C, Barozzi I, Sandoná M, Ryan T, Rojas-Muñoz A, Madaro L, Fasanaro P, et al. 2014. HDAC-regulated myomiRs control BAF60 variant exchange and direct the functional phenotype of fibro-adipogenic progenitors in dystrophic muscles. *Genes & Development* **28**: 841–857.

Sanjana NE, Cong L, Zhou Y, Cunniff MM, Feng G, Zhang F. 2012. A transcription activator-like effector toolbox for genome engineering. *Nat Protoc* **7**: 171–192.

Singh AP, Archer TK. 2014. Analysis of the SWI/SNF chromatin-remodeling complex during early heart development and BAF250a repression cardiac gene transcription during P19 cell differentiation. *Nucleic Acids Research* **42**: 2958–2975.

Sohn DH, Lee KY, Lee C, Oh J, Chung H, Jeon SH, Seong RH. 2007. SRG3 interacts directly with the major components of the SWI/SNF chromatin remodeling complex and protects them from proteasomal degradation. *Journal of Biological Chemistry* **282**: 10614–10624.

Stankunas K, Hang CT, Tsun Z-Y, Chen H, Lee NV, Wu JI, Shang C, Bayle JH, Shou W, Iruela-Arispe ML, et al. 2008. Endocardial Brg1 represses ADAMTS1 to maintain the microenvironment for myocardial morphogenesis. *Developmental Cell* **14**: 298–311.

Subramanian A, Tamayo P, Mootha VK, Mukherjee S, Ebert BL, Gillette MA, Paulovich A, Pomeroy SL, Golub TR, Lander ES, et al. 2005. Gene set enrichment analysis: a knowledge-based approach for interpreting genome-wide expression profiles. *PNAS* **102**: 15545–15550.

Takeuchi JK, Bruneau BG. 2009. Directed transdifferentiation of mouse mesoderm to heart tissue by defined factors. *Nature* **459**: 708–711.

Takeuchi JK, Lou X, Alexander JM, Sugizaki H, n PD-OI, Holloway AK, Mori AD, Wylie JN, Munson C, Zhu Y, et al. 2011. Chromatin remodelling complex dosage modulates transcription factor function in heart development. *Nature Communications* **2**: 187–11.

Thomas R, Thomas S, Holloway AK, Pollard KS. 2017. Features that define the best ChIP-seq peak calling algorithms. *Brief Bioinformatics* **18**: 441–450.

Thompson KW, Marquez SB, Lu L, Reisman D. 2015. Induction of functional Brm protein from Brm knockout mice. *Oncoscience* **2**: 349–361.

Wamstad JA, Alexander JM, Truty RM, Shrikumar A, Li F, Eilertson KE, Ding H, Wylie JN, Pico AR, Capra JA, et al. 2012. Dynamic and coordinated epigenetic regulation of developmental transitions in the cardiac lineage. *Cell* **151**: 206–220.

Wang W, Côté J, Xue Y, Zhou S, Khavari PA, Biggar SR, Muchardt C, Kalpana GV, Goff SP, Yaniv M, et al. 1996a. Purification and biochemical heterogeneity of the mammalian SWI-SNF complex. *The EMBO Journal* **15**: 5370–5382.

Wang W, Xue Y, Zhou S, Kuo A, Cairns BR, Crabtree GR. 1996b. Diversity and specialization of mammalian SWI/SNF complexes. *Genes & Development* **10**: 2117–2130.

Wang Y, Wong RHF, Tang T, Hudak CS, Yang D, Duncan RE, Sul HS. 2013. Phosphorylation and recruitment of BAF60c in chromatin remodeling for lipogenesis in response to insulin. *Molecular Cell* **49**: 283–297.

Yoo AS, Staahl BT, Chen L, Crabtree GR. 2009. MicroRNA-mediated switching of chromatin-remodelling complexes in neural development. *Nature* **460**: 642–646.

Zhou CY, Johnson SL, Gamarra NI, Narlikar GJ. 2016. Mechanisms of ATP-Dependent Chromatin Remodeling Motors. *Annu Rev Biophys* **45**: 153–181.

Figure Legends:

Figure 1. BAF complexes change subunit composition during cardiac differentiation

(A) Schematic representation of cardiac differentiation (B) Isolation of BRG1 complexes by anti-FLAG immunoprecipitation from a non-FLAG tagged mouse ESC line (lane 1) and a Brg1-3x FLAG tagged ESC line differentiated to cardiomyocytes at different stages (lane 2-6). BRG1 complex isolated at CM (lane 6) is shown with increased contrast (lane 7). Protein complexes were loaded in a 10% SDS-PAGE and stained with SyproRuby protein gel stain.

(C) Mass spectrometric analysis of FLAG peptide eluted BRG1 complexes. The peptide intensities are normalized to BRG1 intensities and further normalized across row. Color red and blue indicates enrichment and depletion respectively while white represent unchanged across five different stages (see Supplemental Table S1). (D) BAF complex subunit protein levels were probed from nuclear extracts at different stages of cardiac differentiation. Histone H3 was used as a loading control. (E) Peptide intensities of immune-precipitated and FLAG eluted BAF170 complex isolated from five indicated stages of cardiac differentiation shown after normalized to the levels of BAF170 protein and across the row. Color scheme: blue depleted and red enriched and yellow unchanged across stages. (F) Similar to E, but as BAF60c as a bait protein. Complexes isolated from cardiac precursor and cardiomyocytes and shown after normalization to BAF60c levels. Subunits enriched in CP and CM are shown in the lower panels.

Figure 2. BAF complex composition changes do not affect ATPase or nucleosome repositioning in-vitro

(A) Nucleosome repositioning by BAF complexes isolated at indicated stages of cardiac differentiation. N0 represents the starting nucleosome position. N1-N4 represent BAF displaced repositioned nucleosomes over time. (B) Quantification of nucleosome positioning. Error bars represent s.e.m of two independent replicates. (C) Nucleosome stimulated ATP hydrolysis by BAF complexes isolated at different stages of cardiac differentiation. Error bars represent s.e.m of three independent replicates

Figure 3. BRG1 differentially affects district set of genes at cardiac precursors

(A&C) Significantly affected (≥1.5 fold, $p<0.05$) genes from three independent biological replicates in cardiac precursors (A) and cardiac myocytes(C). Selected up and down regulated genes are in yellow and black boxes respectively. (B&D) Gene ontology (GO) enrichment terms are represented for up and down regulated genes in cardiac precursors (B) and cardiac myocytes (D).

Figure 4. BRG1, BAF60c and BAF170 show common as well as divergent transcriptional effects

Comparison of genes that are significantly affected (≥ 1.5 fold, p-value<0.05) in any one genotype over the corresponding wild type in cardiac precursors (A) or cardiomyocytes (B). Clustering of the genes are shown in vertical colored bars to the left. Representative genes involved in various biological processes are shown to right of the heat-map. (C) Number of genes significantly deregulated (≥1.5 fold, $p<0.05$) in cardiac precursor cells in either Brg1 conditional KO or constitutive KO of *Baf60* or *Baf170* were compared to their WT counterparts and plotted in a Venn diagram. (D) same as C**,** except in cardiomyocytes. BRG1 regulated

genes show decreased overlap in cardiomyocytes than cardiac precursors with both BAF60c and BAF170 regulated genes.

Figure 5. BAF60c and BAF170 regulate stoichiometry of BRG1 associated factors

(A) BRG1 complexes isolated in absence of BAF60c (lanes 2-7) or BAF170 (lanes 8-11). Lane 1 shows complexes similarly isolated from cardiac precursors in an untagged strain. (B&C) Peptide intensities of immune-precipitated and FLAG eluted BRG1 complex in absence of either BAF170 (B) or BAF60c (C) subunits shown after normalization to the levels of BRG1 protein and across row isolated from cardiac precursors and cardiomyocytes. Blue and red indicate depletion and enrichment respectively while white and yellow indicate minimal changes in peptide intensities. Lower panels show subunits enriched or depleted at least 1.25 fold in each of these conditions.

Figure 6. BRG1 occupancy co-relates with cardiac transcription factor binding

(A**)** BRG1 binding aligned over transcriptional start sites (TSS) of ensemble genes (left panel) and active enhancers marked by acetylation of lysine 27 residues of histone 3 (right panel) and over the TSS of 545 genes that are deregulated in absence of *Brg1*(B). (C) BRG1 ChIPSeq track is compared over input DNA track at the TSS and regulatory regions of BRG1 activated (Tbx5, Myocd) and repressed (Rdh10) genes in cardiac precursors. (D) Enriched biological process in genes that are activated or repressed by Brg1 and within 1Mb of Brg1 binding sites. (E) Enriched biological process in genes that are activated or repressed repressed by Brg1 that overlap with genes nearest to active CP enhancers. Motifs enriched in BRG1 binding sites associated with BRG1 activated genes (F) and repressed genes (G). GATA4 (H) and TBX5 (I) binding correlates well over BRG1 binding sites in cardiac precursor.

Figure 7. BAF170 regulates BRG1 complex genomic expulsion

(A) BRG1 binding remains unchanged in WT and delta BAF170 at the 4791 BRG1 peaks in cardiac precursors (B) BRG1 binding at the same 4791 CP peaks is severely reduced in WT and BAF60c KO cardiomyocytes, however retained in BAF170 KO cardiomyocytes.

Materials and Methods

Mouse ES cell culture

Mouse embryonic stem cells (ESCs) were cultured in feeder free condition in DMEM+ glutamax (ThermoFisher, 10566) media supplemented with 15% fetal bovine serum (Hyclone, SH30071.03), 10^3 U/ ml leukemia inhibitory factor (Millipore, ESG1107), 2mM glutamine, 13mM 2-mercaptoethanol (Life Tech. 21985-023), 0.1mM non-essential amino acids (Life Tech, 11140-050), 0.1mM sodium pyruvate (LifeTech, 11360), and 1x Pencillin/Sreptomycin (LifeTech, 15140-122). ESCs were cultured in gelatinized tissue culture flasks. TrypLE (ThermoFisher, 12563011) was used to dissociate cells and followed by quenching in DMEM media with 10% FBS. Cells were passages every 2 days with daily media changes.

Knockout cell line generation

BAF60c was inactivated by targeting exon 2 of *Baf60c* gene with two pairs of TALENs following Sanjana et. al (Sanjana et al. 2012) except a CAGGS promoter replacing the CMV promoter (Giorgetti et al. 2014). The TALEN's targets are as follows: GCCCCCTAAGCCCTCTCCAGAGAACATCCAAGCTA GAATGACTTGGTCGCTGCTAC and CCCGCCCCTCTCCAAGACCCTGGGTTGGTA ACCCTGCGCTGAGCGATGAGTGGGAG

BAF170 was targeted using CRISPR/Cas9 with sgRNA targeting Exon 2 of *Baf170* gene following the protocol in Congo et al.(Cong et al. 2013). sgRNA were cloned to Bbs1 digested pX330 vector by annealing the following primers 5' caccg CGCACCGCTTACTAAACTGC 3' and

5' aaac GCAGTTTAGTAAGCGGTGCG c **3'** (lowercase to create Bbs1 digestion site). Targeting vector was constructed by cloning 458 and 459bp of Baf170 DNA upstream and downstream of midpoint of sgRNA target site into Kpn1-Xho1 and BamH1-Not1 sites of pFPF (derivative of Addgene Plasmid #22687, Neomycin is replaced with Puromycin cassette).

Plasmids were prepared using maxiprep kit (Macherey-nagel), ethanol precipitated and DNA suspended in TE.

For transfection, 2.5ug of each of TALEN Baf60c plasmids were used. For BAF170 knockout, 2.5ug sgRNA plasmid and 20ug of BAF170 targeting constructs were used. Plasmids were transfected by microporation using the Neon system (Thermofisher) using a 100uL tip with 1 million cells at 1400V, 10ms and 3 pulses. Cells were grown for 48 hours and then serially diluted and grown either in absence (for BAF60c) or presence of puromycin (for BAF170) for 8-10days. Single colonies were picked manually and transferred to 96 well tissue culture plates coated with 0.1% gelatin and passaged 2-3 times and replica plated. Cells were then PCR genotyped from one replicate of plates to confirm loss of exon2 (*Baf60c*) or insertion of puromycin cassette (*Baf170*). Further, amplified DNA around the regions was sequenced to confirm mutation.

Cardiomyocyte differentiation

Cardiomyocyte differentiation were performed as described previously(Kattman et al. 2011; Wamstad et al. 2012). Briefly, ES cell (70-80% confluence) were harvested and resuspendend ($7.5x10^5$ cells/ml) in EB media (75% v/v Iscove's modification of DMEM (Corning, 15-016-CV), 25% v/v Ham's F-15 (Corning, 15-080-CV), 0.5% each of N2 supplement (ThermoFisher, 17502048), B27 without vitamin A(ThermoFisher, 12587010), 0.5% BSA (Sigma Aldrich, A9576-50ml), 1x glutamine (Gibco, 25030-081), 1x Penicillin/streptomycin (ThermoFisher, 15140-122)

and supplemented just before use with ascorbic acid (1mM) and monothioglycerol (400uM)). The cells were grown into embroid bodies (EBs) for two days in ultra-low attachment suspension culture dishes (Corning, 430591). Embroid bodies (EBs) were dissociated using TrpLE and resuspendend in EB media containing 5ng/ml of hVEGF(R&D Systems, 293-VE-050), 8ng/ml Activin-A (R&D Systems, 338-AC-050) and 0.1 to 1.6ng/ml Bmp4(R&D Systems, 314-BP-010, usually a range of Bmp4 concentrations optimized for each cell line) in ultralow suspension culture dishes for 40hrs. EBs were dissociated and cultured in in monolayers in StemProP34 media (ThermoFisher, 10639011) containing 0.2mM L-Glutamine, 0.1 mg/ml ascorbic acid, 5ng/ ml VEGF, 10ng/ ml FGF basic (233-FB-025) and 25ng/ ml FGF 10 (R&D Systems 345-FG-025) for 6 days. Beating cardiac myocytes were observed day 6 onwards and efficiency of differentiation was measured by antibody staining of cardiac troponin T followed by immunofluorescence and fluorescence activated cell sorting (FACS). BRG1 was deleted as described earlier (Alexander et al. 2015). Briefly, $Brg1^{fl/fl}$;Actin-CreER ESCs (Ho et al. 2009a; 2011) were differentiated and cultures were treated with 200 nM 4-hydroxytamoxifen (4-OHT) diluted from a 5 mg/ml stock solution in tetrahydrofuran (THF) or with only THF for control, 48 hrs. before the desired deletion.

Nuclear extract preparation, western blot and anti-FLAG immunoaffinity purification

Nuclear extract were prepared using protocol describe before (Abmayr et al. 2006). Briefly, cells were harvested, washed twice in ice cold PBS, washed once with hypotonic buffer (10 mM HEPES, pH 7.9, 1.5 mM $MgCl_2$, 10 mM NaCl with 0.2 mM PMSF and 0.5 mM DTT added immediately before use) and incubated in 5 cell volume of hypotonic buffer for 15 min in ice. Cells were homogenized 15 times using a dounce, lysis checked with trypan blue staining and nuclei collected after centrifuging 3000g for 5 mins. Nuclei were suspended in 1 volume of

nuclear lysis buffer (20 mM HEPES, pH 7.9, 25% glycerol, 1.5 mM $MgCl_2$, 0.3 M NaCl, 0.02%, NP40, 0.2 mM EDTA, with 0.2 mM PMSF and 0.5 mM DTT added immediately before use) and incubated at 4°C in rotating condition. Supernatant were collected as nuclear extract after centrifuging 25,000g for 30min at 4°C. Western blotting was performed using standard techniques. Briefly, nuclear extract was diluted, boiled and resolved by electrophoresis. Protein was transferred to a PVDF membrane followed by blocking with Odessey blocking buffer (Licor, 927-40000) for 1 hr followed by desired primary antibody diluted in blocking buffer with 0.1% Tween 20, overnight at 4°C. Membranes were washed in TBST and stained with compatible secondary antibody in blocking buffer containing 0.1% Tween 20 and 0.02% SDS. After antibody staining, membranes were washed and imaged in a Odessy Fc imaging system (LI-COR). Primary antibodies used were anti-Brg1 (Abcam, ab110641, 1:1000), anti-FLAG (Sigma, F1804, 1:1000) and anti-BAF155 (Bethyl, A301-021A, 1:1000), anti-BAF170 (Bethyl, 1:1000, A301-39A), anti-BAF60c (Cell Signaling Technologies, 62265, 1:0000) and anti-H3 (SantaCruz,sc-86541:1000). Secondary antibodies used are Donkey anti-rabbit IRDye 800cw (Licor, 926-32213, 1:10,000), Donkey anti-mouse IRDye 800cw (Licor, 925-32212, 1:10,000), Donkey anti-goat IRDye 680cw (Licor, 925-68074-1:10,000).

For immunoaffinity purification of BAF complexes, cells were grown, differentiated and harvested at specific stages of cardiac differentiation. Nuclear extract was made from 10^8 cells as described above except the final clearing was at 100,000g for 1hr. Nuclear extract were incubated with 50ul of anti-FLAG M2 agarose gel (Sigma, A2220) at 4°C rotating overnight. Bead bound protein complexes were washed 10 times with 1ml of nuclear extract buffer supplemented with protease inhibitor (Sigma Aldrich, 5892970001). Proteins was competitively eluted by incubating with 0.1mg/ml FLAG peptides (ELIM Biopharmaceutical) four times in 50ul of nuclear extraction buffer containing 100mM NaCl. The protein complexes were resolved in

10% SDS PAGE and stained with SyproRuby protein gel stain (ThermoFisher, S12000).

Masspectrometry

Protein complexes were digested with trypsin for LC-MS/MS analysis. Samples were denatured and reduced in 2M urea, 10 mM NH4HCO3, 2 mM DTT for 30 min at 60° C, then alkylated with 2 mM iodoacetamide for 45 min at room temperature. Trypsin (Promega) was added at a 1:100 enzyme:substrate ratio and digested overnight at 37° C. Following digestion, samples were concentrated using C18 ZipTips (Millipore) according to the manufacturer's specifications. Desalted samples were evaporated to dryness and resuspended in 0.1% formic acid for mass spectrometry analysis.

Digested peptide mixtures were analyzed by LC-MS/MS on a Thermo Scientific LTQ Orbitrap Elite mass spectrometry system equipped with a Proxeon Easy nLC 1000 ultra high-pressure liquid chromatography and autosampler system. Samples were injected onto a C18 column (25 cm x 75 um I.D. packed with ReproSil Pur C18 AQ 1.9um particles) in 0.1% formic acid and then separated with a one-hour gradient from 5% to 30% ACN in 0.1% formic acid at a flow rate of 300 nl/min. The mass spectrometer collected data in a data-dependent fashion, collecting one full scan in the Orbitrap at 120,000 resolution followed by 20 collision-induced dissociation MS/MS scans in the dual linear ion trap for the 20 most intense peaks from the full scan. Dynamic exclusion was enabled for 30 seconds with a repeat count of 1. Charge state screening was employed to reject analysis of singly charged species or species for which a charge could not be assigned.

Raw mass spectrometry data were analyzed using the MaxQuant software package (version 1.3.0.5)(Cox and Mann 2008). Data were matched to the SwissProt mouse protein sequencess (downloaded from UniProt on 7/19/2016). MaxQuant was configured to generate and search

against a reverse sequence database for false discovery rate (FDR) calculations. Variable modifications were allowed for methionine oxidation and protein N-terminus acetylation. A fixed modification was indicated for cysteine carbamidomethylation. Full trypsin specificity was required. The first search was performed with a mass accuracy of +/- 20 parts per million and the main search was performed with a mass accuracy of +/- 6 parts per million. A maximum of 5 modifications were allowed per peptide. A maximum of 2 missed cleavages were allowed. The maximum charge allowed was 7+. Individual peptide mass tolerances were allowed. For MS/MS matching, a mass tolerance of 0.5 Da was allowed and the top 6 peaks per 100 Da were analyzed. MS/MS matching was allowed for higher charge states, water and ammonia loss events. The data were filtered to obtain a peptide, protein, and site-level FDR of 0.01. The minimum peptide length was 7 amino acids. Results were matched between runs with a time window of 2 minutes for technical duplicates. All precursor (MS1) intensities of valid peptide matches were quantified by the Maxquant LFQ algorithm using the match between runs option to minimize missing values.

For statistical analysis, the quantitative change of peptides that were uniquely assigned to protein isoforms across all IPs were compared with the MSstats R package (v. 2.3.4)(Choi et al. 2014). Briefly, all peak intensities were Log_2-transformed and their distributions were median-centered across all runs using the scale option. All remaining missing intensity values were imputed by setting their value to minimal intensity value per run, as an estimate for the MS Limit Of Quantitation. The normalized dataset was then analyzed by fitting a mixed effects model per protein using the model without interaction terms, unequal feature variance and restricted scope of technical and biological replication. The average change (Log2-Fold-Change) of the model-based abundance estimate was computed by comparing replicates of each differentiation stage against the ES undifferentiated pool. Proteins with a greater than four fold change (Log2 Fold Change > 2) and test p-value < 0.05 were determined as significantly altered during differentiation.

Nucleosome reconstitution, repositioning and ATPase assay

Recombinant *Xenopus laevis* histone octamers were constituted on a 601-nucleosome positioning DNA(Lowary and Widom 1998) as described (Hota et al. 2013). Briefly, 601 DNA containing mononucleosomes were assembled at 37C with 8-10ug of recombinant octamers, 100-200 fmol of ^{32}P-labelled DNA, 10ug of unlabeled homogenous DNA and 1.8M NaCl in a 10ul reaction. Samples were serially diluted to a final concentration of ~300mM NaCl. Nucleosome assemblies were analyzed on a 4% native polyacrylamide gel (acrylamide:bisacrylamide; 35.36:1) in 0.5x Tris-Borate-EDTA buffer at 4°C. For nucleosome repositioning assay, 5.8nM homogenous nucleosomes with 30 and 60bp overhangs (30-nuc-60) were incubated with 1nM BAF enzymes and excess ATP (1mM) for increasing amount of time (0, 2, 6, 18 and 54min) at 30°C. Reaction was quenched in presence of 16.6mM γ-S-ATP. Repositioned nucleosome was separated from starting nucleosomes in a 5% native polyacrylamide gel in 0.2x Tris-Borate EDTA buffer at 4°C. The gel was dried and exposed and imaged acquired in a Typhoon Phosphorimager (GE) and quantified using Optiquant (GE). ATPase assays were performed by adding 800nM (γ-32P) ATP to bound nucleosome-BAF complexes and incubating for increasing times (0 to 128 mins). ATP and free phosphate were separated by thin layer chromatography on polyetheleneimine-cellulose(Thomas Scientific, 2738E80).

RNA-Sequencing

ES cell-derived cardiac precursors or cardiomyocytes (n=3 for each genotype) were harvested for RNA extraction using miRNeasy micro kit with on-column DNase I digestion (Qiagen). Total RNA was isolated from 1.5-2×10^6 cells using TRIzol reagent. RNA-seq libraries were prepared with the Ovation RNA-seq system v2 kit (NuGEN). With this method, mRNA is reverse

transcribed to synthesize first-strand cDNA with random hexamers and a poly-T chimeric primer. Following second strand synthesis double-stranded DNA is then amplified using single primer isothermal amplification (SPIA). Libraries from the SPIA amplified cDNA were made using the Ultralow DR library kit (NuGEN). RNA-seq libraries were analyzed by Bioanalyzer and quantified by QPCR (KAPA). High-throughput sequencing was done using a HiSeq 2500 instrument (Illumina). RNA reads were aligned with TopHat2(Kim et al. 2013), counts per gene calculated using featureCounts (Liao et al. 2014)and edgeR (Robinson et al. 2010) was used for the analysis of differential expression. Differential expressed RNAs were analyzed at cardiac precursor (D5.3) and cardiac myocyte (D10) stages of differentiation. RNAs that showed significant differential expression between wild type and nulls (p-value <0.05) and also changed more than 1.5-fold in nulls over wild type at a specific stage of differentiation were selected for analysis, avoiding duplicate and redundant entries. K-means clustering and pheatmap functions in R were used to cluster FKM values of selected RNAs and generate heat maps respectively.

GO enrichment analysis were performed in GO RILLA(http://cbl-gorilla.cs.technion.ac.il/) and visualized in REVIGO (http://revigo.irb.hr/).

ChIP-Seq

Chromatin immunoprecipitation of BRG1 in WT, ΔBAF60c and ΔBAF170 were performed according to O'Geen et al. (O'Geen et al. 2011) with modifications, in biological duplicate for CP and one replicate for CM but with samples combined from two biological replicates. Briefly, cells at CP and CM of cardiac differentiation were harvested and crosslinked with 2mM disuccinimidyl gulatarate (DSG) for 45 mins, washed twice with PBS, followed by crosslinking with 1% formaldehyde for 15 mins. Cells were quenched with 0.125M glycine for 5 mins, washed in PBS thrice and stored at -80°C. Frozen pellet of dual crosslinked cells ($5x10^7$) were thawed, washed in PBS and lysed in PBS containing 1% triton X for 3 mins in ice followed by 25 cycles of dounce with a tight pestle. Nuclei were collected and washed once with MNase digestion buffer

(50mM Tris.cl, pH7.6, 1mM $CaCl_2$, 0.2% Triton X, 5mM Sodium Butyrate with 1x protease inhibitor and 0.5mM PMSF added just before use) at 350g for 5mins. Nuclei were digested with 400U of micrococcal nuclease (ThermoFisher, 88216) for exactly 5 mins at 37°C. MNase digestion was stopped by adding stop buffer (10mM EDT, 10mM EGTA and 0.1% SDS). Chromatin were sonicated for short time (2 cycles, 30s ON, 1 min OFF at output 4 in a VirSonic sonicator), centrifuged at 10,000g for 10mins and supernatant stored at -80°C. Extent of MNase digestion was measured by agarose gel electrophoresis. Chromatin (40ug) was diluted to 5 fold in IP dilution buffer (50mM Tris.Cl, pH7.4, 150mM NaCl, 1% NP-40, 0.25% Sodium deoxycholate, 1mM EDTA) without EDTA and pre-cleared with 25ul of M-280 goat anti-rabbit IgG dyna beads (ThermoFisher, 11203D) for 2 hrs followed by addition with 1ug of anti-Brg1 antibody (Abcam, 110641) for 12-16hrs. 5% of samples were set aside as input before antibody addition. Antibody bound BRG1-DNA complexes were Immunoprecipitated using 25ul of M-280 goat anti-rabbit IgG dyna beads for 2hrs, washed twice with IP dilution buffer, five times with IP wash buffer(100 mM Tris.Cl, pH 9.0, 500mM Lithium chloride, 1% NP-40 and 1% Sodium deoxycholate) and thrice with IP wash buffer containing 150mM NaCl. DNA was eluted with 200ul of elution buffer (10mM Tris.Cl, pH 7.5, 1mM EDTA and 1%SDS), NaCl was added to both ChIP and input samples (0.52M) and crosslinking reversed for 6 – 12 hrs at 65°C. Samples were digested with RNase A, and proteinase K in presence of 3ug of glycogen, and DNA purified with Ampure beads (Beckman Coulter, A63881) and eluted in 50ul of TE. To prepare libraries for ChIP Sequenceing, DNA were end repaired, A-tailed followed by adapter ligation (Illumina TrueSeq) and 14 cycles of PCR amplification. PCR amplified DNA was size selected (200 -400bp) followed by gel extraction (Qiagen) and eluted in 20ul TE. The concentration and size of eluted libraries was measured (Qubit and Bioanalyzer) before sequencing in a NEBNextSeq sequencer.

Reads (single end 75bp) were trimmed using fastq-mcf and aligned to mouse genome mm9 assembly using Bowtie(Langmead et al. 2009). Minimum mapping quality score was set to 30. Statistically enriched bins with a P-value threshold set to $1x10^{6}$ were determine with input DNA serving as the background model (Thomas et al. 2017). UCSC genome browser was used to generate the browser tracks. Galaxy (https://usegalaxy.org/) was used to pool multiple replicates to generate browser tracks and tornado plots. GREAT (http://bejerano.stanford.edu/great/public/html/) was used to generate gene lists near BRG1 binding sites.

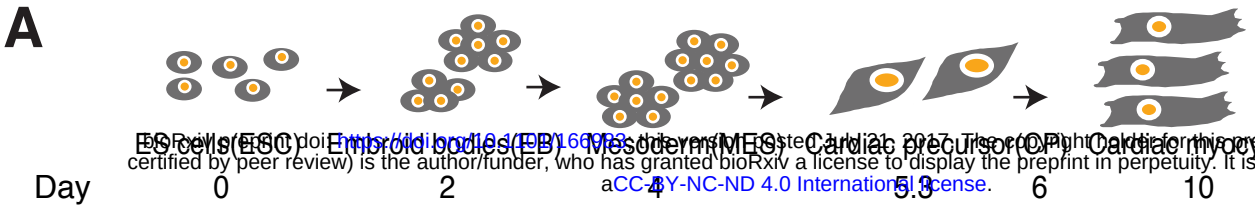

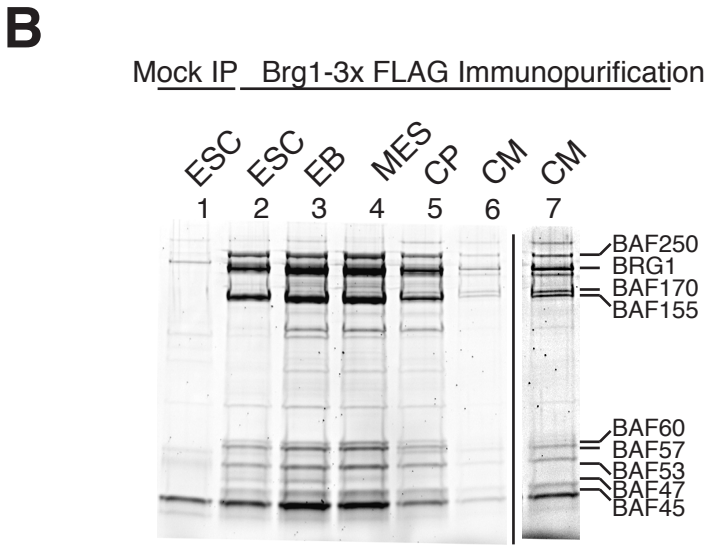

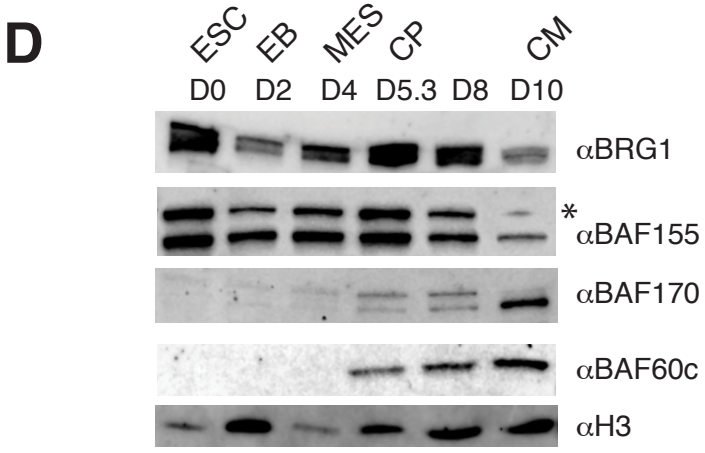

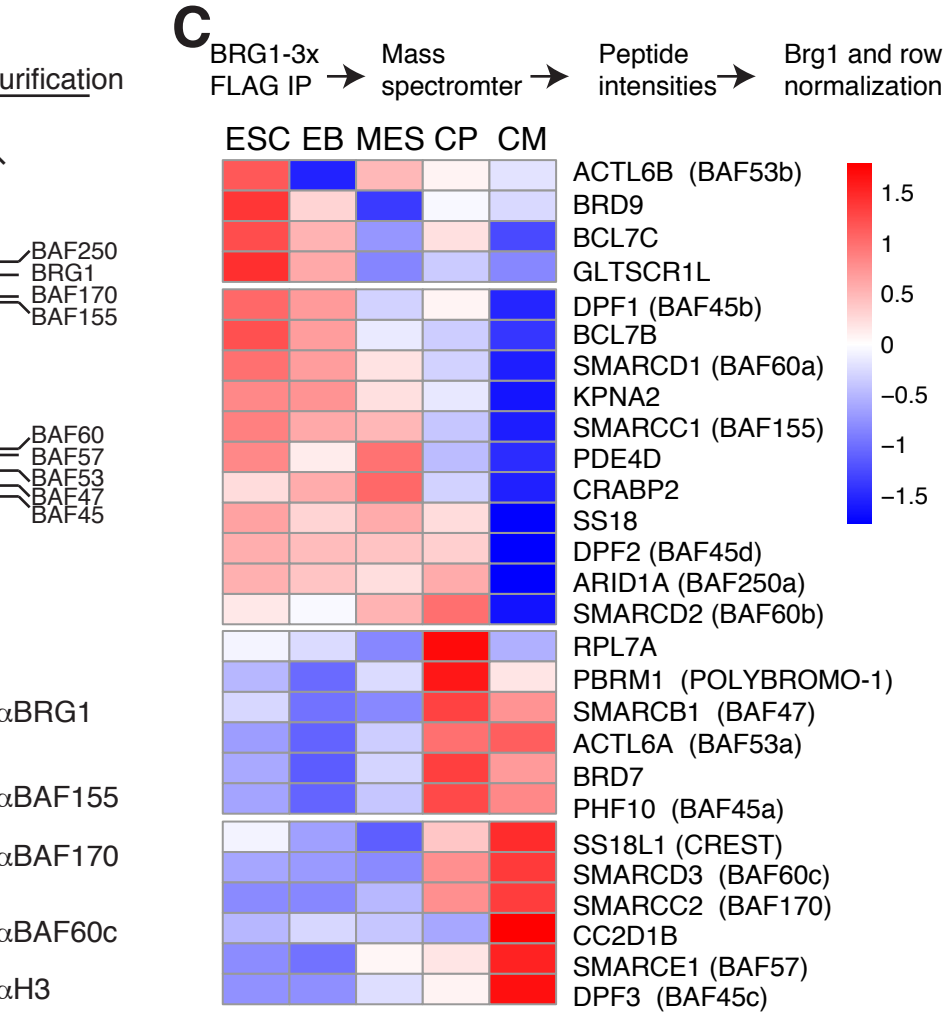

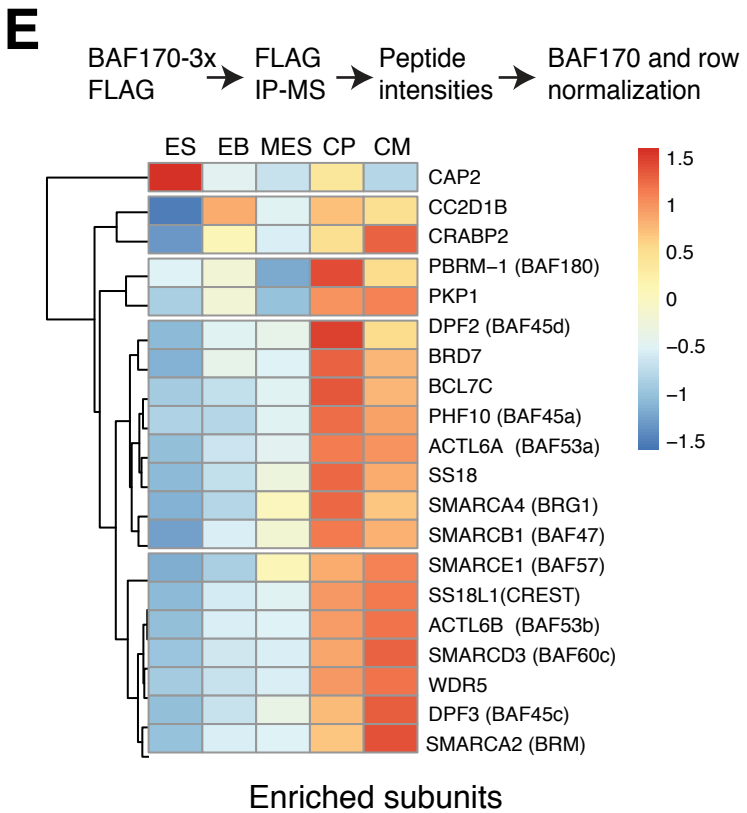

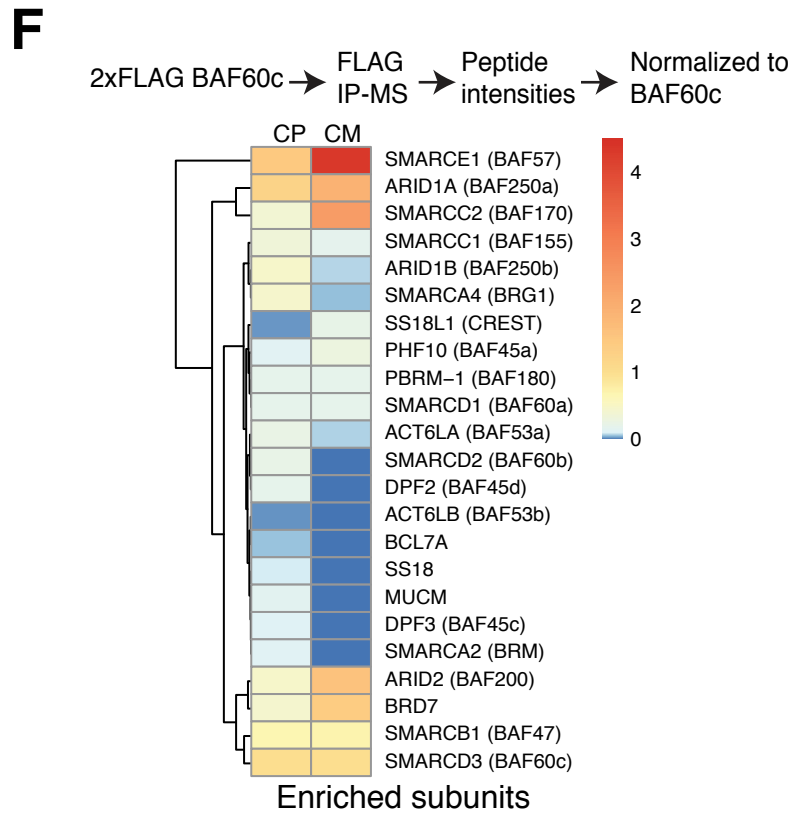

Enriched subunits

CP	CM
BAF180, BAF45a & d, BRD7 BCL7c, SS18, BRG1, BAF47	CRABP2, BAF57, CREST,BAF53b, BAF60c, WDR5, BAF45c, BRM

Enriched subunits

CP	CM
BAF57, BAF250a &b, BAF200 BRD7, BAF47, SS18	BAF57, BAF250a, BAF170 BAF200, BRD7, BAF47, CREST

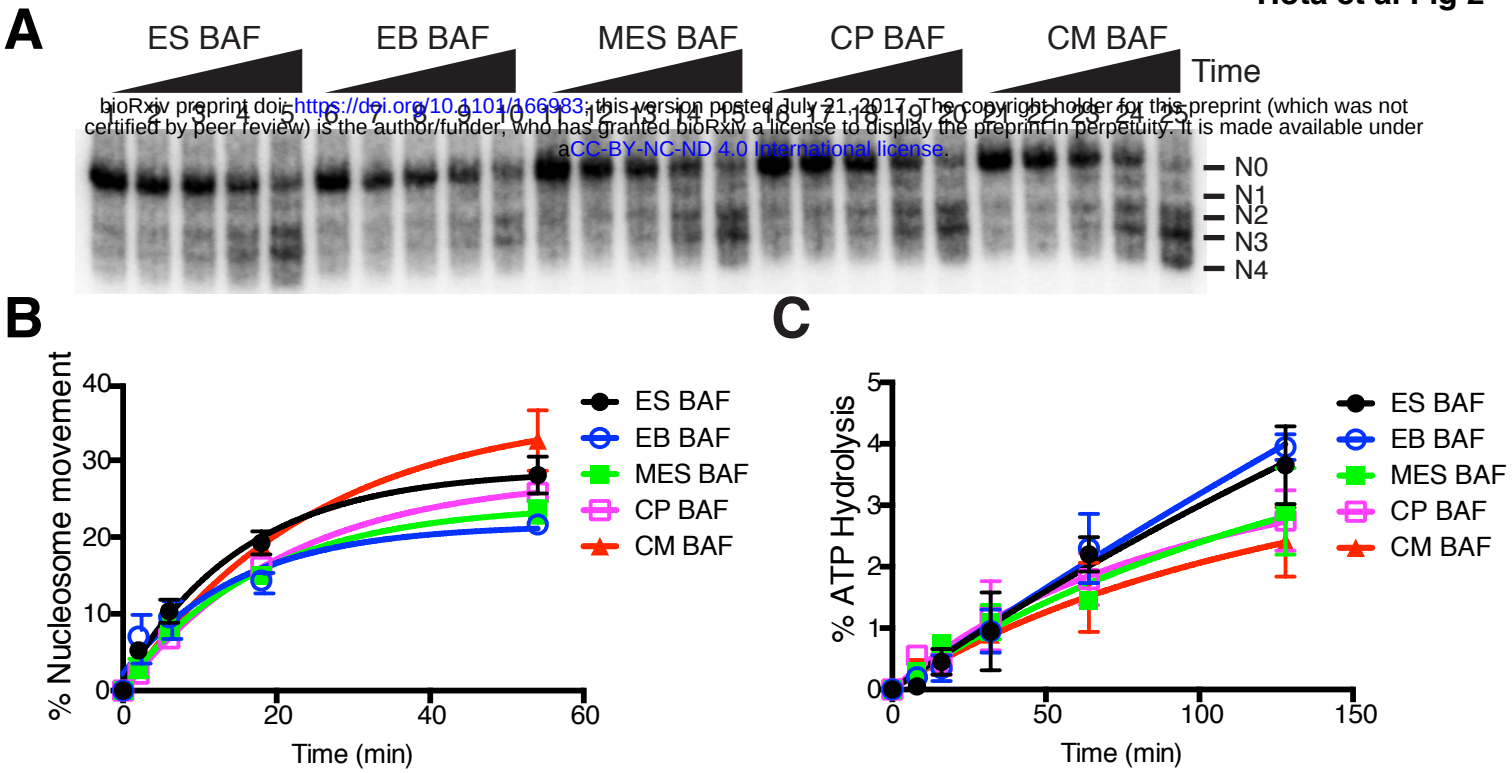

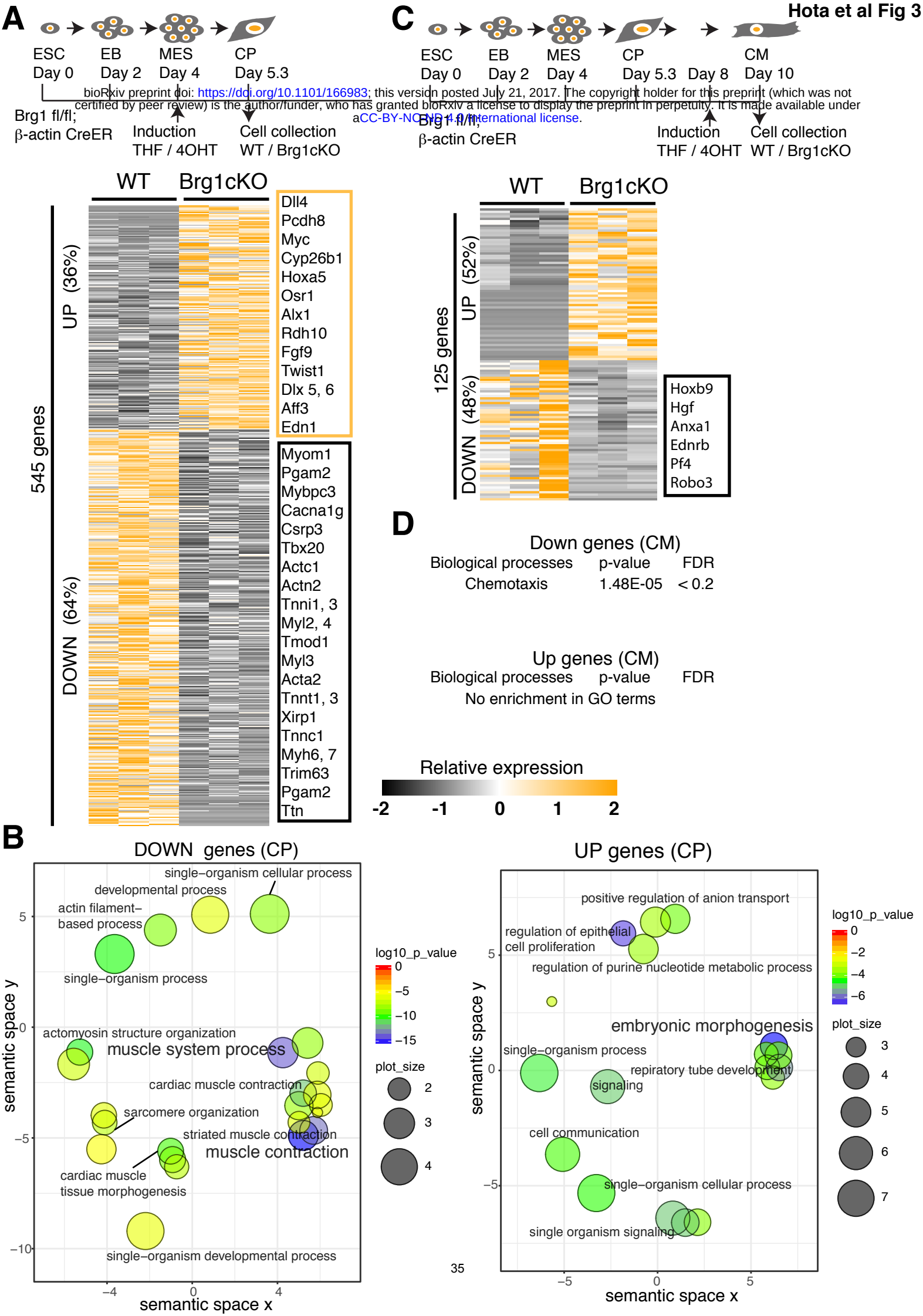

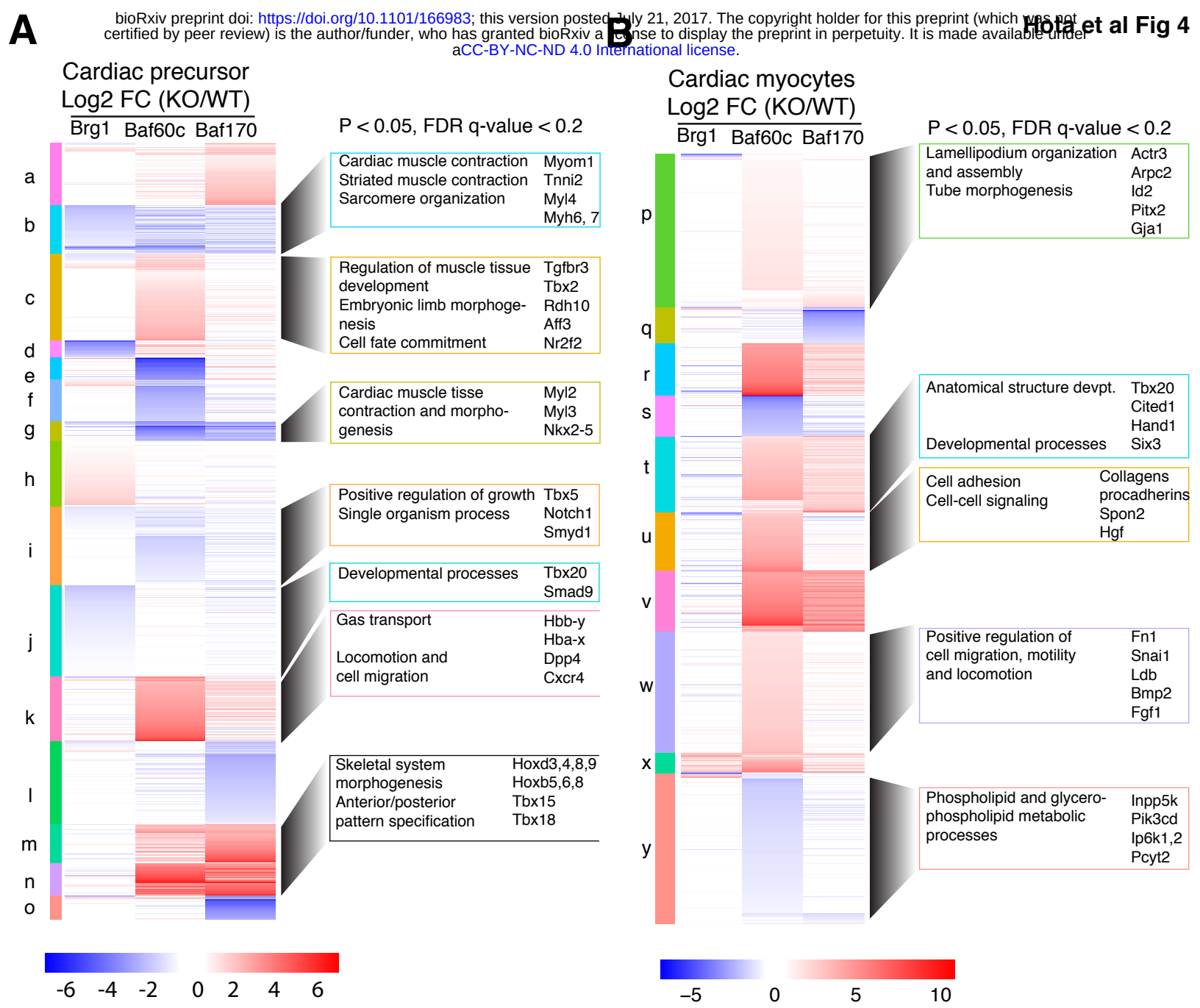

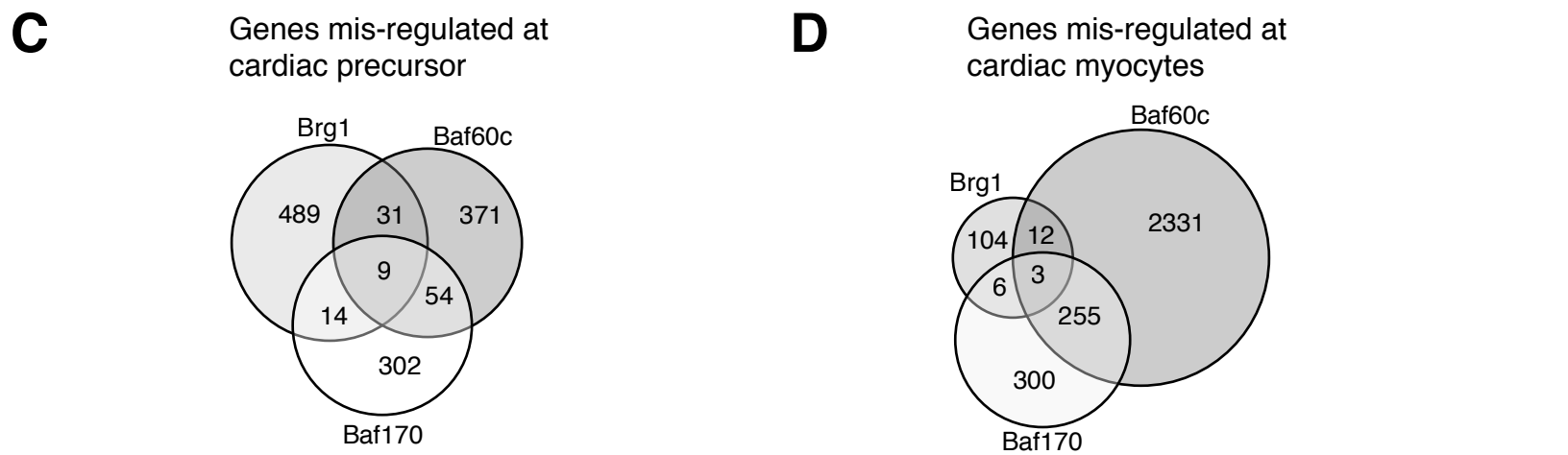

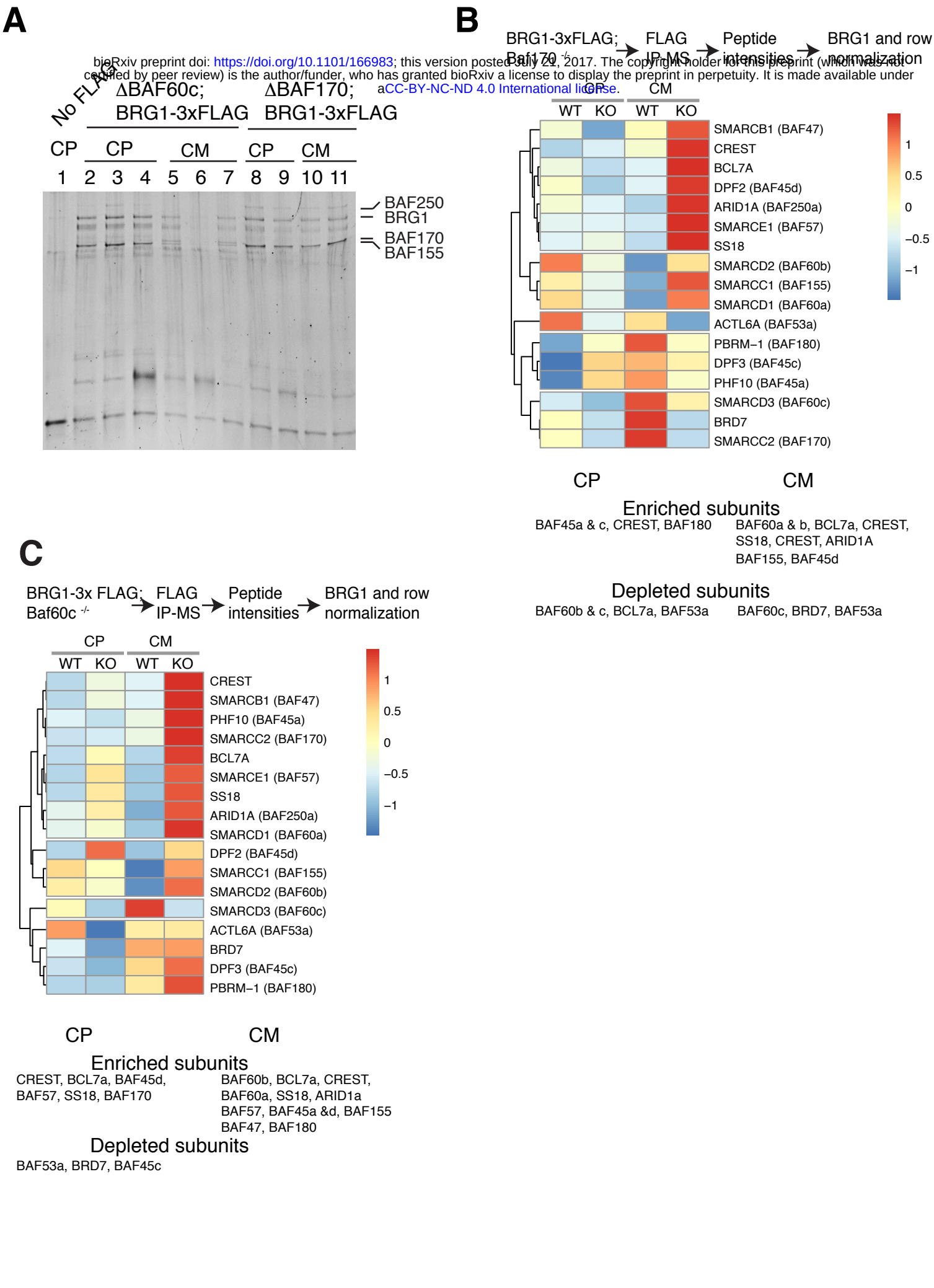

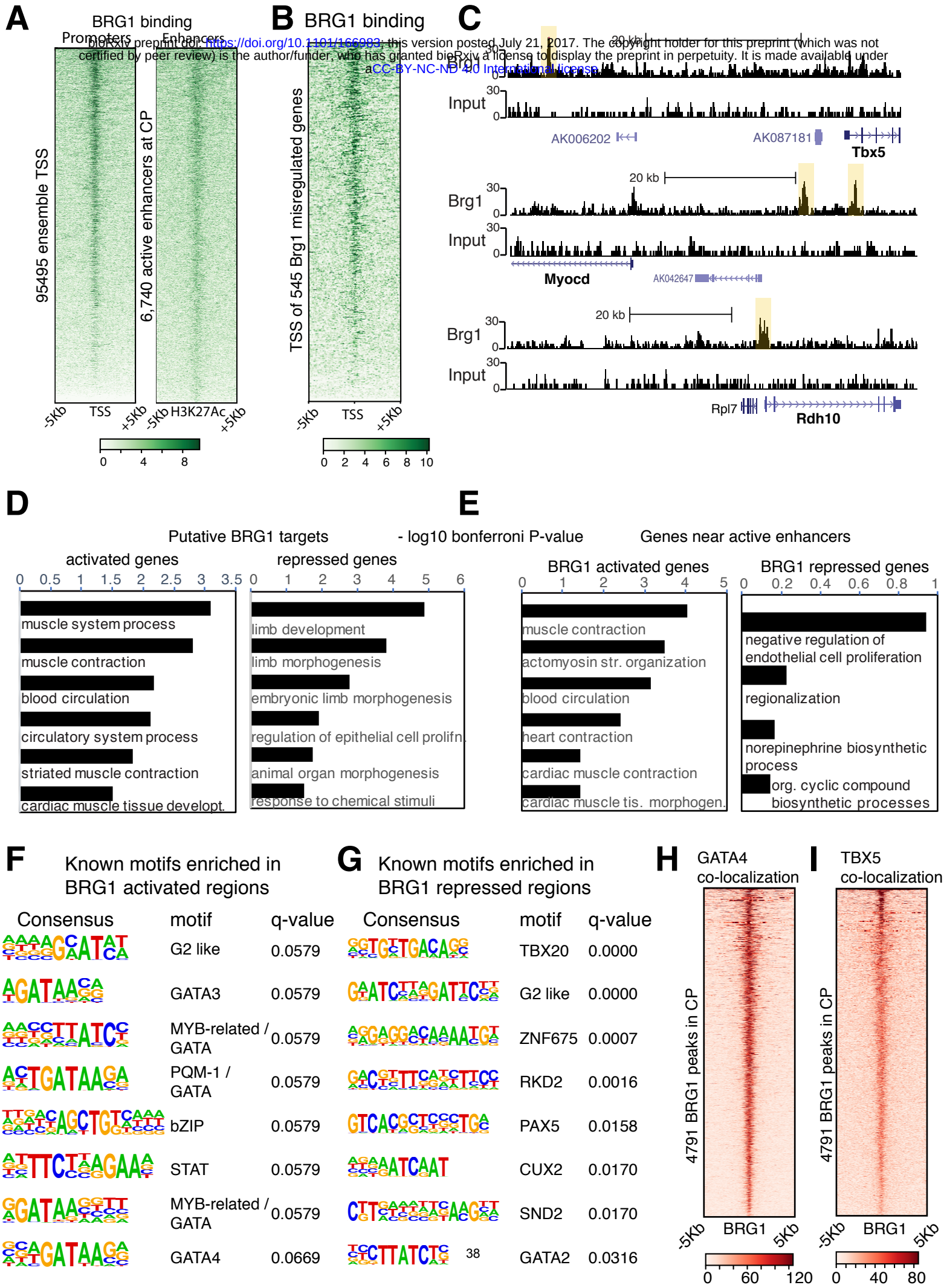

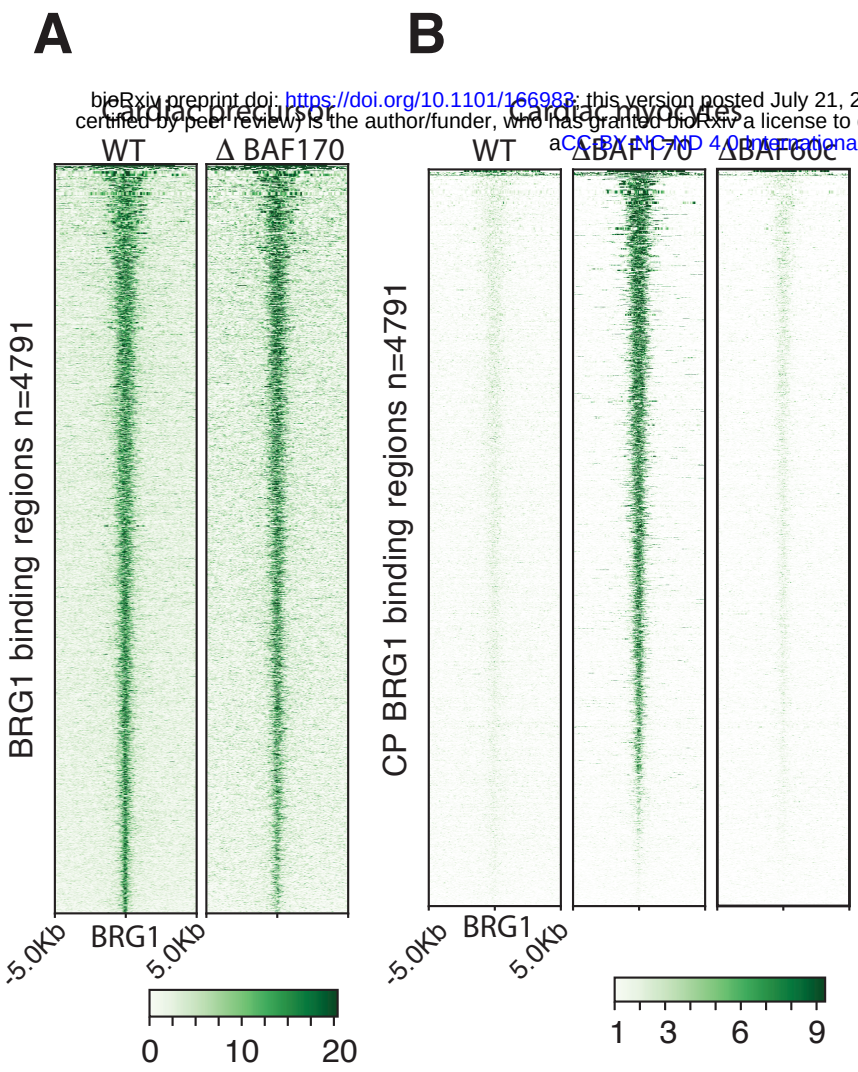

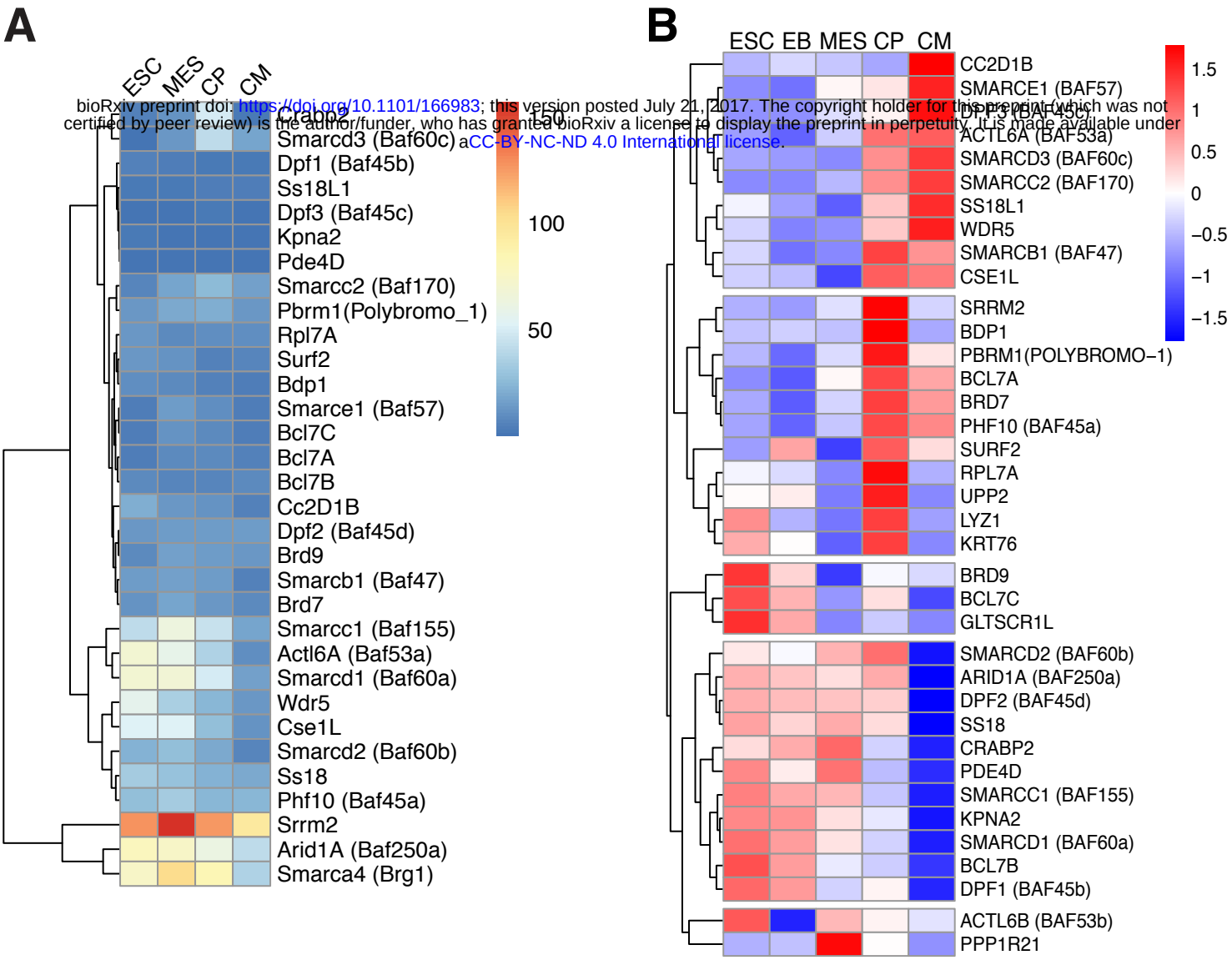

Supplemental Figure S1. Gene expression analysis of BAF subunits (related to Fig. 1 and Fig. 3)

(A) BRG1 associated factor subunits identified from masspectrometry were analyzed for gene expression across four indicated stages of cardiomyocyte differentiation using previously published RNASeq (Wamstad et al., 2012). Color bar indicates normalized RPKM values. (B) BRG1 associated proteins at indicated stages of cardiac differentiation. Peptide intensities are plotted after normalized to the intensities of bait protein BRG1 and further normalized across all the stages (row normalized). Color bar indicate relative intensities of proteins with blue and red indicating depletion and enrichment of subunits across different stages of differentiation respectively.

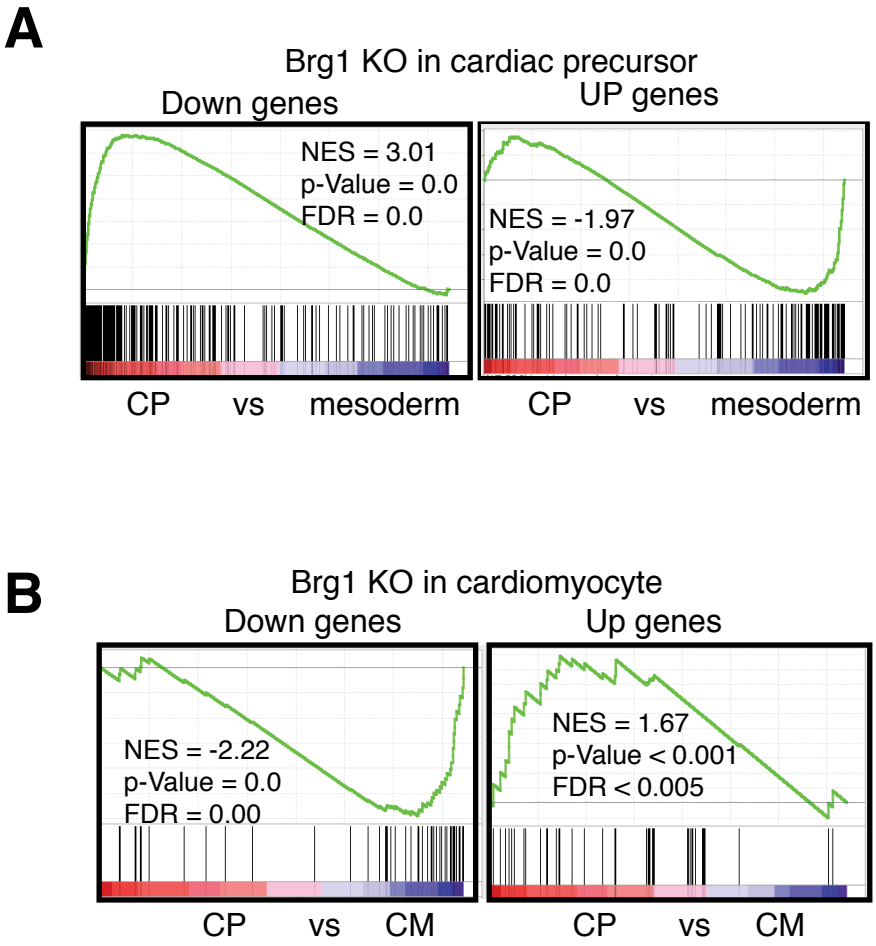

Supplemental Figure S2. Gene set enrichment analaysis (GSEA) of Brg1 regulated genes at CP and CM (related to Fig. 3)

(A,B) Gene set enrichment (GSEA) analysis of genes down regulated or up regulated in absence of *Brg1* at cardiac precursors (A) or cardiomyocytes (B). CP and CM denote cardiac precursor and cardiac myocytes respectively, NES denotes normalized enrichment score.

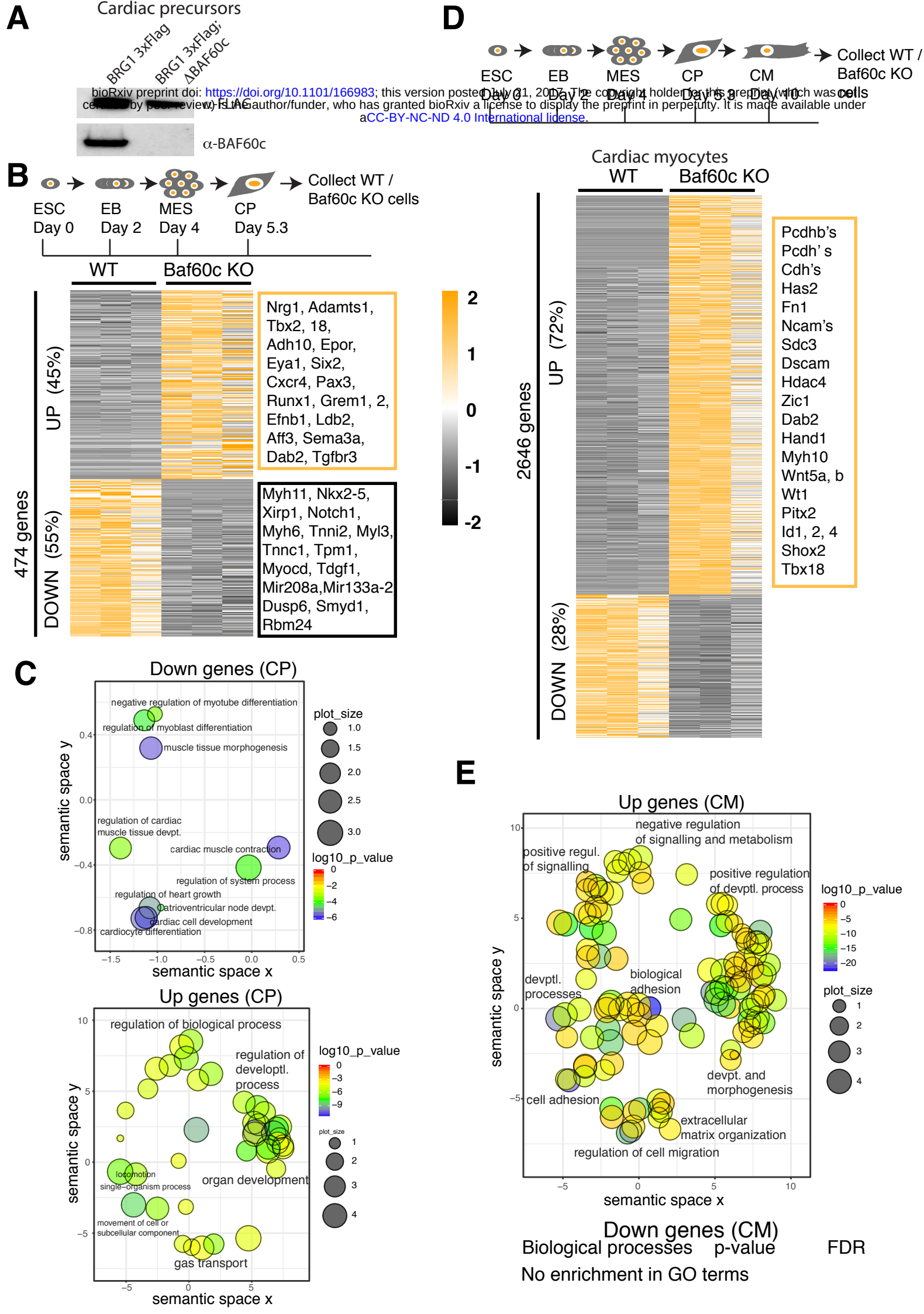

Supplemental Figure S3. Transcriptional analysis of loss of *Baf60c* at cardiac precursor and cardiomyocytes (related to Fig. 4)**.**

(A) Cardiac precursor cells containing 3xFLAG tag at the c-terminus of BRG1 in presence (WT) or absence of BAF60c (ΔBAF60c) were probed with α-FLAG (sigma) or α-BAF60c (Cell Singlaing Technologies) antibodies. (B) Upper panel: Schematics depicting time of cell collection from WT and *Baf60c* KO cells. Lower panel: Normalized FPKM values of RNA expression from three independent biological replicates of significantly (≥1.5 fold, $p<0.05$) deregulated genes in WT and BAF60c KO in cardiac precursor. Example genes upregulated or down regulated in absence of BAF60c are represented in yellow and black boxes respectively. (C) GO biological process enrichment of genes downregulated (upper panel) or up-regulated (lower panel) in absence of BAF60c. (D and E) Same as B and C except in cardiac myocytes. Color bar indicates relative gene expression with black and yellow representing repressed and activated respectively.

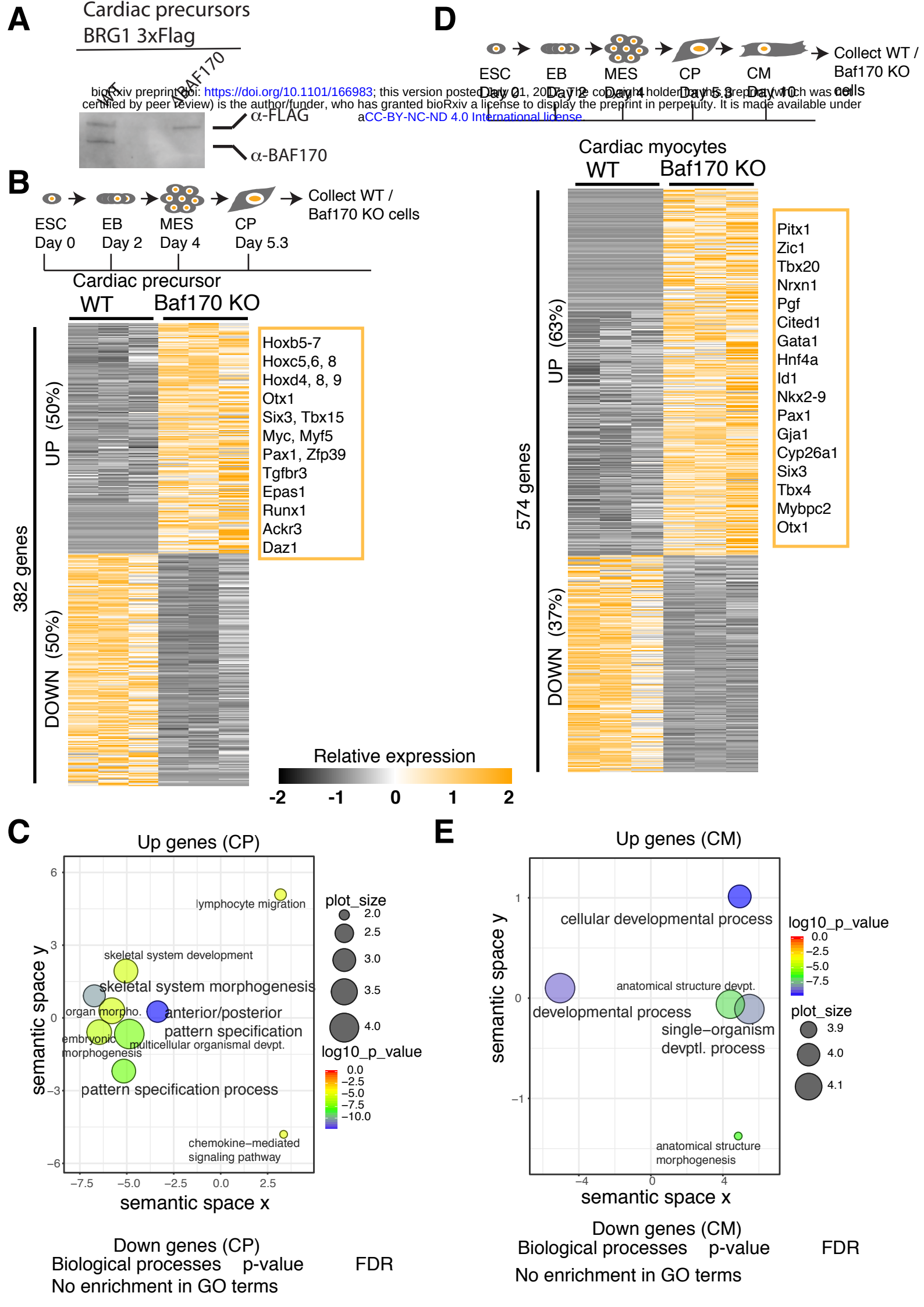

Down genes (CP)
Biological processes p-value FDR
No enrichment in GO terms

Down genes (CM)
Biological processes p-value FDR
No enrichment in GO terms

Supplemental Figure S4. Transcriptional analysis of loss of *Baf170* at cardiac precursor and cardiomyocytes (related to Fig. 4).

Same as in Figure S4, except analyzed for the loss of BAF170. Anti-BAF170 antibody (Bethyl Labs) was used for the western blot.

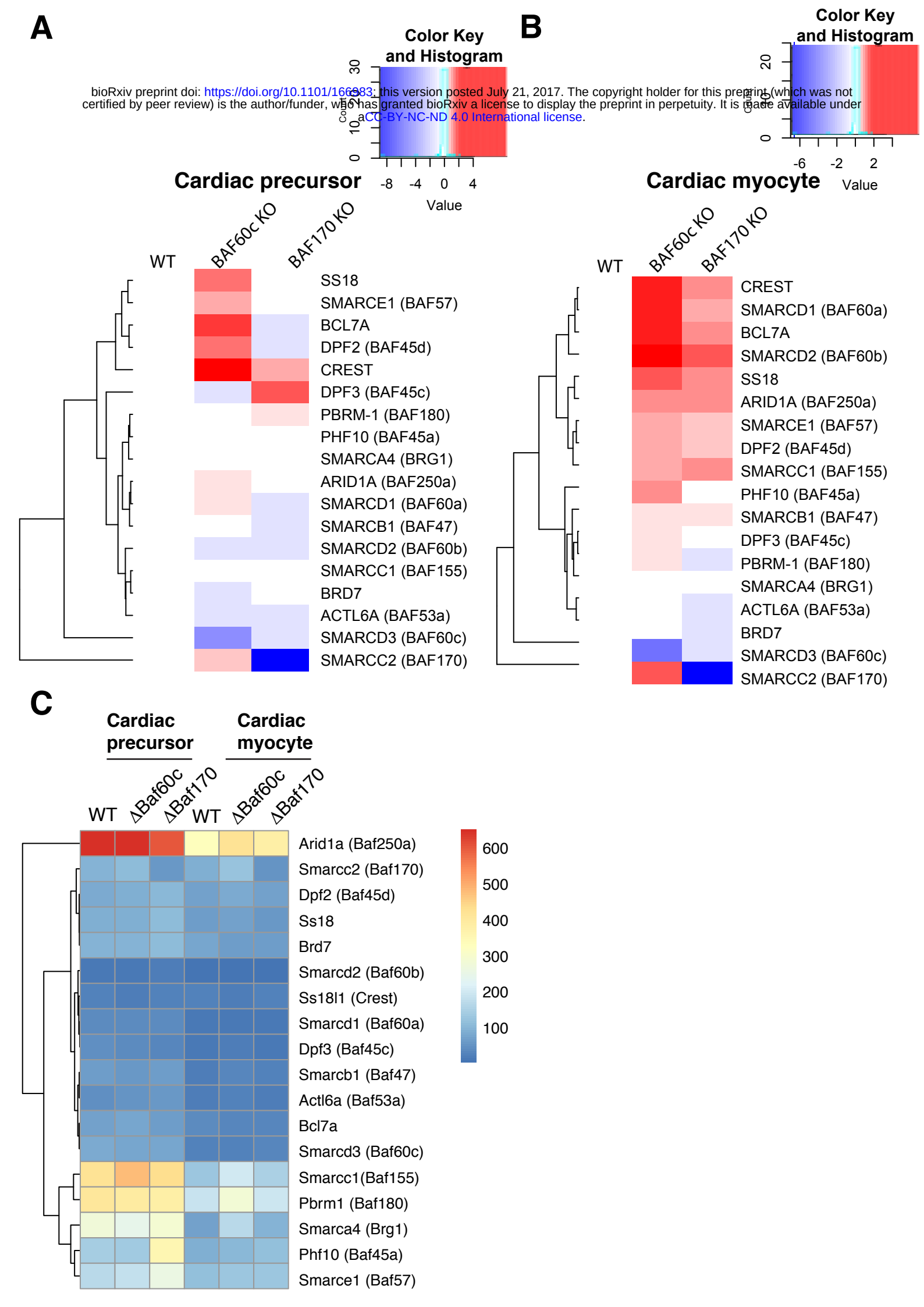

Supplemental Figure S5. Proteomic and transcriptional analysis of BRG1 associated subunits in absence of either BAF60c or BAF170 (related to Fig. 5)

(A) BRG1 complexes from cardiac precursor cells lacking BAF60c or BAF170 are normalized to the protein levels of BRG1 in each genotype and to their WT counterparts. (B) Same as A, except in cardiomyocytes. Color bar indicates relative association of proteins with BRG1 with blue, white and red representing depletion (less than 1.25-fold), no change (within 1.25-fold) and enrichment (more than 1.25-fold change) in protein abundance respectively. (C) Gene expression analysis of BRG1 associated subunits at the indicated stages in absence of BAF60c or BAF170 were plotted for the indicated genotypes at CP and CM. Color bar shows the normalized median FPKM expression values from three biological replicates.

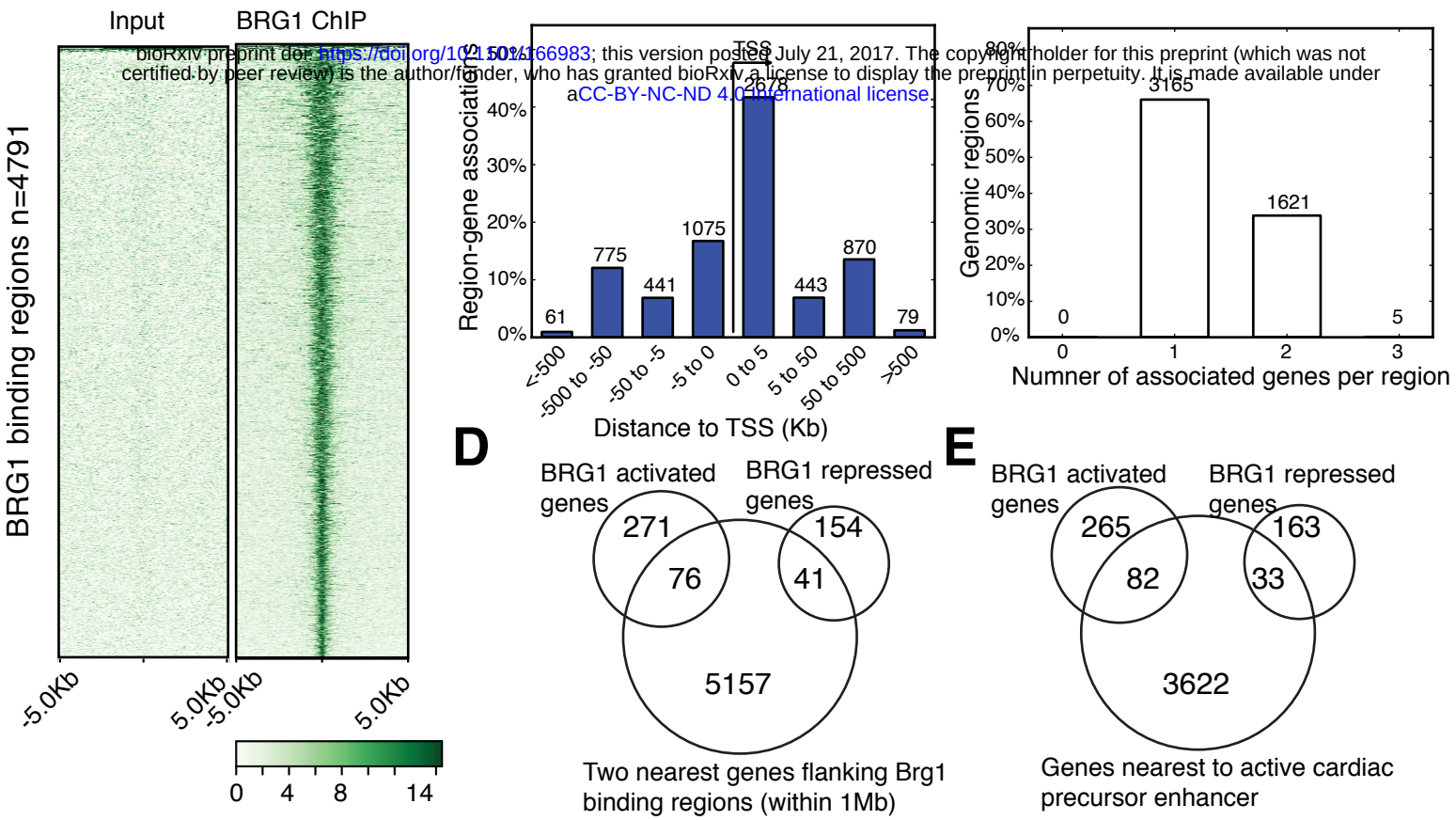

Supplemental Figure S6. Genome-wide binding of BRG1 by ChIPSeq in cardiac precursor cells (related to Fig. 6)

(A**)** Tornado plot showing input and BRG1 binding over 4791 binding sites identified in cardiac precursors. (B) BRG1 binding region with respect to TSS of genes generated by GREAT. (C) BRG1 binding regions and their gene association within 1 mega base regions (D) Venn diagram showing the overlap between genes flanking BRG1 binding (within 1Mb) and genes either down or up regulated in absence of Brg1. (E) overlap between nearest gene to active enhancers in cardiac precursor and genes either down or up regulated in absence of Brg1.

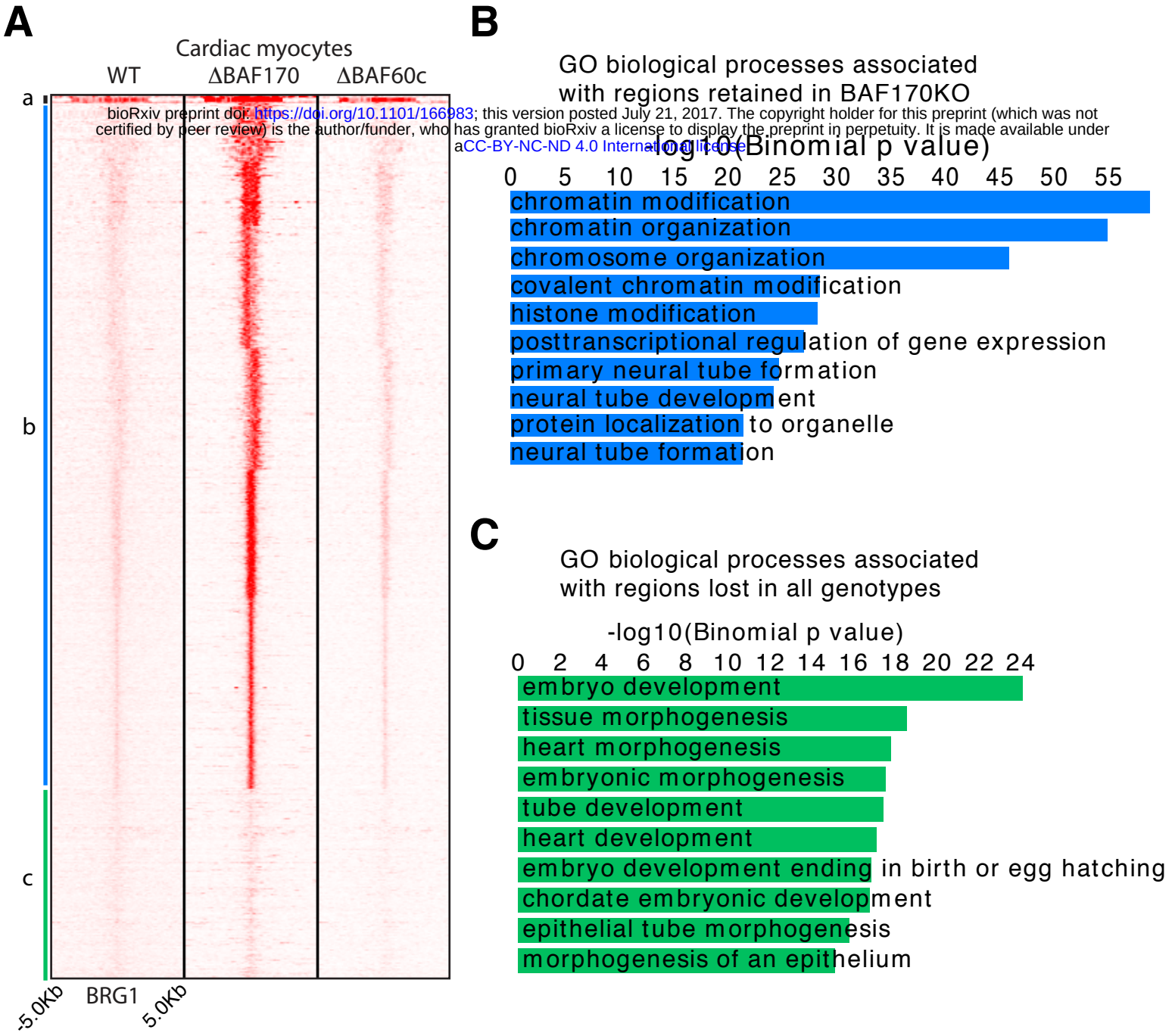

Supplemental Figure S7. BAF170 regulates eviction of BRG1 complexes from large number of genomic site in cardiomyocytes (related to Figure 7)

(A) BRG1 ChIPSeq signal measured at 4791 cardiac precursors specific BRG1 binding sites and clustered. A small number of sites (31 out of 4791) show BRG1 binding in WT, BAF170 KO and BAF60c KO (cluster a). BRG1 binding disappears in 1019 sites (cluster c), however largely retained in absence of BAF170 (at 3741 sites). GO biological process analysis of nearby genes (within 1 megabase) of sites retained in absence of BAF170 (B) or evited in all geneotypes (C) are shown.